

PARAMETER-ROBUST UZAWA-TYPE ITERATIVE METHODS FOR DOUBLE SADDLE POINT PROBLEMS ARISING IN BIOT'S CONSOLIDATION AND MULTIPLE-NETWORK POROELASTICITY MODELS

Q. HONG, J. KRAUS, M. LYMBERY, AND F. PHILO

ABSTRACT. This work is concerned with the iterative solution of systems of quasi-static multiple-network poroelasticity (MPET) equations describing flow in elastic porous media that is permeated by single or multiple fluid networks. Here, the focus is on a three-field formulation of the problem in which the displacement field of the elastic matrix and, additionally, one velocity field and one pressure field for each of the $n \geq 1$ fluid networks are the unknown physical quantities. Generalizing Biot's model of consolidation, which is obtained for $n = 1$, the MPET equations for $n \geq 1$ exhibit a double saddle point structure.

The proposed approach is based on a framework of augmenting and splitting this three-by-three block system in such a way that the resulting block Gauss-Seidel preconditioner defines a fully decoupled iterative scheme for the flux-, pressure-, and displacement fields. In this manner, one obtains an augmented Lagrangian Uzawa-type method, the analysis of which is the main contribution of this work. The parameter-robust uniform linear convergence of this fixed-point iteration is proved by showing that its rate of contraction is strictly less than one independent of all physical and discretization parameters.

The theoretical results are confirmed by a series of numerical tests that compare the new fully decoupled scheme to the very popular partially decoupled fixed-stress split iterative method, which decouples only flow—the flux and pressure fields remain coupled in this case—from the mechanics problem. We further test the performance of the block triangular preconditioner defining the new scheme when used to accelerate the GMRES algorithm.

1. INTRODUCTION

In this paper we propose and analyze stationary iterative methods for solving the equations of multiple network poroelastic theory (MPET) which describe flow in deformable porous media. The latter is modeled as an elastic solid matrix comprising $n \geq 1$ superimposed fluid networks with possibly vastly varying characteristic length scales and hydraulic conductivities, see e.g., [52] and the references therein.

Dual-porosity/dual-permeability models have been proposed and studied in a geomechanical context, see, e.g. [8, 7], providing a generalization of Biot's consolidation model which is obtained for $n = 1$, see [12, 13]. Over the last decade, the MPET equations have gradually gained attention as a tool for modeling flow across scales and networks in soft tissue. Biological multicompartamental poroelasticity models can be used to embed more specific medical models, e.g., to describe water transport in the cerebral environment and explore the pathogenesis of acute and chronic hydrocephalus [51], or to study effects of obstructing cerebrospinal fluid (CSF) transport and to demonstrate the impact of aqueductal stenosis and fourth ventricle outlet obstruction (FVOO) [54, 53], or to find medical indications of oedema formation [20].

Recently, the MPET model has also been used in order to gain a better understanding of the processes involved with the mechanisms behind Alzheimer's disease (AD), the most common form of dementia [25]. Most prominently, the so-called amyloid hypothesis states that the accumulation of neurotoxic amyloid- β ($A\beta$) into parenchymal senile plaques or within the walls of arteries is a basic cause of this disease. In [24], a partial validation of a four-network poroelastic model for metabolic waste clearance is presented in a qualitative way, i.e., by showing a qualitative agreement of

2010 *Mathematics Subject Classification.* 65M12, 65M60, 65F10, 65N22, 35Q92.

the cerebral blood flow (CBF) data obtained from arterial spin labeling (ASL) images and the corresponding model output for different regions of the brain. Although the authors of these papers conclude that there is a need for more experimental and clinical data to optimize the boundary conditions and parameters used in numerical modeling, they also stress the potential of MPET modeling as a testing bed for hypotheses and new theories in neuroscience research.

Regarding the numerical solution of the MPET equations mainly two different approaches have been investigated in the last couple of years. The first one has been proposed in [38] and uses a mixed finite element formulation based on introducing an additional total pressure variable. Energy estimates for the continuous solutions and a priori error estimates for a family of compatible semidiscretizations demonstrate that this formulation is robust for nearly incompressible materials, small storage coefficients, and small or vanishing transfer between networks.

The second approach is based on a generalization of the classical three-field formulation of Biot's model and explicitly accommodates Darcy's law for each fluid network. This formulation enforces the exact conservation of mass at the price of including additionally n vector fields for the Darcy velocities (fluxes). A parameter-robust stability analysis of this flux-based MPET model has been presented in [28] along with fully parameter-robust norm-equivalent preconditioners. Following [27, 32], the authors propose in [28] a family of strongly conservative locking-free discretizations for the MPET model and establish the related optimal error estimates for the stationary problems arising from implicit time discretization by the backward Euler method. These results also cover the case of vanishing storage coefficients.

Various works can be found on discretizations and efficient iterative solvers and preconditioning techniques for the quasi-static Biot model addressing two-field, see, e.g. [14, 1], three-field, see, e.g., [45, 31, 37, 27], and four-field formulations, see, e.g., [36, 6].

Two of the most popular and likely most efficient iterative schemes for solving the equations of poroelasticity are the so-called undrained split and fixed-stress split iterative methods, which, contrary to the drained split and the fixed-strain split methods, are unconditionally stable, see [33]. The first convergence analysis of the former methods has been presented in [44] for the quasi-static Biot system. Subsequent refined results focus mostly on variants of the fixed-stress method addressing multirate fixed-stress split iterative schemes [2], fully discrete iterative coupling of flow and geomechanics [3], heterogeneous media and linearized Biot's equations [16], two-grid fixed-stress schemes for heterogeneous media [22], or space-time finite element approximations of the quasi-static Biot system [9]. A strategy for optimizing the stabilization parameter in the fixed-stress split iterative method for the Biot problem in two-field formulation has been presented in [50].

The fixed-stress method has also been recently successfully used in combination with Anderson acceleration for the solution of non-linear poromechanics problems [17]. Moreover, monolithic and splitting based solution schemes have been considered and analyzed for solving quasi-static thermo-poroelasticity problems with nonlinear convective transport [19]. The latter work focuses on the analysis of fully and partially decoupled schemes for heat, mechanics and flow applied to the linearized problem obtained via the so-called L -scheme. All previously mentioned works, in presence of flux and pressure unknowns, solve the flow equations implicitly, i.e., as a coupled subsystem, a strategy which we will not pursue in this paper.

A desirable property of preconditioners, in addition to their uniformity with respect to discretization parameters, is their robustness regarding potentially large variations of the physical parameters. This task can be studied in the framework of operator preconditioning on the level of the continuous model, cf. [43]. Targeting Biot's consolidation model the parameter-robustness of norm-equivalent preconditioners has been established in [37] for the total-pressure based formulation and in [27] for the classical three-field formulation based on displacement, Darcy velocity and fluid pressure fields. Both approaches have been generalized to the MPET model, see [38, 28].

One potential advantage of the approach presented in [28] is exact mass conservation. A disadvantage, however, is that the presence of n fluxes and n associated pressures makes the system in general more difficult and also more time-consuming to solve. The fixed-stress split iterative method has recently been generalized to be applicable not only to the Biot ($n = 1$) but also to the more general MPET ($n \geq 1$) systems in [29] which presents a fully parameter-robust convergence analysis and determines a close to optimal acceleration parameter.

However, in the conservative approach obtained from generalizing the classical three-field formulation of Biot's model, the block of n unknown fluxes (with d components each) couples to a block of n pressure unknowns creating a subsystem with $n(d + 1)$ scalar quantities of interest as compared to the $(n(d + 1) + d)$ unknown scalar functions in the whole system. Hence, considering the above-mentioned four-network model ($n = 4$) in three space dimensions ($d = 3$), for example, this results in a flux-pressure subsystem with approximately 16/19 of the size of the whole system. This explains why a further decoupling of the flux from the pressure block of unknowns in an iterative method is of particular interest in this approach.

The goal of the present paper is to propose and analyze a class of fully decoupled iterative schemes, which contrary to the fixed-stress split iterative method also decouple the *flux-pressure* subsystem. In this respect, it can be seen as a continuation of the analysis presented in [29].

As already mentioned, the target problem is a three-by-three block system with a double saddle point. The abstract canonical form of the operator (matrix) of the related operator equation can be represented in the form

$$(1.1) \quad \begin{bmatrix} A_1 & 0 & B_1^T \\ 0 & A_2 & B_2^T \\ B_1 & B_2 & -C \end{bmatrix}$$

with A_1 and A_2 being symmetric positive definite (SPD) operators and C a symmetric positive semidefinite (SPSD) operator. The operator (1.1) defines a double saddle point problem and can be rearranged in such a way that it has the form

$$(1.2) \quad \begin{bmatrix} A_1 & B_1^T & 0 \\ B_1 & -C & B_2 \\ 0 & B_2^T & A_2 \end{bmatrix}$$

and thus fits the definition of a multiple saddle point operator as given in [49] where block-diagonal Schur complement preconditioners for multiple saddle point problems of block tridiagonal form are analyzed. We will use a combined augmentation and splitting technique to construct in a block Gauss-Seidel framework fully decoupled augmented Lagrangian Uzawa-type methods for linear systems with an operator (matrix) of the canonical form (1.1). Although our methodical approach to construct preconditioners is similar to the one taken in the recent works [10, 11], see also [56], there are also major differences. Firstly, the double saddle point problems considered in [10, 11] are generated by operators of the canonical form

$$(1.3) \quad \begin{bmatrix} A_1 & B_1^T & B_2^T \\ B_1 & 0 & 0 \\ B_2 & 0 & -C \end{bmatrix}$$

with A_1 being SPD and C being SPSPD. It can easily be seen that the operators (1.1) and (1.3) are of a different type in the sense that they can not be transferred one into the other by permutations of rows and columns. The second main difference is that the analysis in [10, 11] uses arguments from classical linear algebra whereas our convergence proofs use techniques from functional analysis aiming at quantitative bounds that might be useful when applying the proposed iterative methods at the level of finite element approximations of the continuous problems.

The remainder of the paper is organized as follow: In Section 2, we first formulate the MPET problem, introduce the notation and transform the problem into a coupled system with a double saddle point operator of the form (1.2). Based on this notation we then recall the fixed-stress split iterative method in a block Gauss-Seidel framework. It follows the construction of a new class of fully decoupled iterative Uzawa-type methods, which requires an additional augmentation step. This section ends with summarizing some preliminary and auxiliary results that are used in the convergence analysis of the new class of methods presented in Section 3. The numerical tests in Section 5 serve the assessment of the performance of the iterative methods and preconditioners developed in this paper comparing them also with the fixed-stress split iterative method analyzed in [29].

2. ITERATIVE COUPLING METHODS FOR THE MPET PROBLEM

2.1. The MPET system - formulation and notation. Consider the quasi-static MPET equations in a bounded Lipschitz domain $\Omega \subset \mathbb{R}^d$, $d = 2, 3$:

$$(2.1a) \quad \mathbf{v}_i + K_i \nabla p_i = \mathbf{0} \quad \text{in } \Omega \times (0, T), \quad i = 1, \dots, n,$$

$$(2.1b) \quad -\alpha_i \operatorname{div} \dot{\mathbf{u}} - \operatorname{div} \mathbf{v}_i - c_{p_i} \dot{p}_i - \sum_{\substack{j=1 \\ j \neq i}}^n \beta_{ij} (p_i - p_j) = g_i \quad \text{in } \Omega \times (0, T), \quad i = 1, \dots, n,$$

$$(2.1c) \quad -\operatorname{div} \boldsymbol{\sigma} + \sum_{i=1}^n \alpha_i \nabla p_i = \mathbf{f} \quad \text{in } \Omega \times (0, T).$$

The unknown physical quantities in this system are the displacement field \mathbf{u} , the seepage velocities, or fluxes, \mathbf{v}_i , and the scalar pressure fields p_i . The effective stress and strain tensors are given by

$$(2.2) \quad \boldsymbol{\sigma} = 2\mu \boldsymbol{\epsilon}(\mathbf{u}) + \lambda \operatorname{div}(\mathbf{u}) \mathbf{I} \quad \text{and} \quad \boldsymbol{\epsilon}(\mathbf{u}) = \frac{1}{2}(\nabla \mathbf{u} + (\nabla \mathbf{u})^T),$$

respectively with the Lamé parameters λ and μ defined via the modulus of elasticity E and the Poisson ratio $\nu \in [0, 1/2)$ as follows:

$$\lambda := \frac{\nu E}{(1 + \nu)(1 - 2\nu)}, \quad \mu := \frac{E}{2(1 + \nu)}.$$

In (2.1), α_i denote the Biot-Willis coefficients, K_i the hydraulic conductivities, which in this paper for convenience only, are scalars defining the tensor coefficients $\mathbf{K}_i = K_i \mathbf{I}$, c_{p_i} the constrained specific storage coefficients. Considering the right-hand sides in (2.1c) and (2.1b), \mathbf{f} denotes the body force density whereas g_i represent the fluid extractions or injections, see e.g. [48] and the references therein. The parameters $\beta_{ij} = \beta_{ji}$, $i \neq j$ couple the network pressures and are called network transfer coefficients.

By substituting the expression for the stress tensor from (2.2) in (2.1c) the MPET system takes the form:

$$(2.3a) \quad \mathbf{v}_i + K_i \nabla p_i = \mathbf{0}, \quad i = 1, \dots, n,$$

$$(2.3b) \quad -\operatorname{div} \mathbf{v}_i - c_{p_i} \dot{p}_i - \sum_{\substack{j=1 \\ j \neq i}}^n \beta_{ij} (p_i - p_j) - \alpha_i \operatorname{div} \dot{\mathbf{u}} = g_i, \quad i = 1, \dots, n,$$

$$(2.3c) \quad \sum_{i=1}^n \alpha_i \nabla p_i - 2\mu \operatorname{div} \boldsymbol{\epsilon}(\mathbf{u}) - \lambda \nabla \operatorname{div} \mathbf{u} = \mathbf{f}.$$

After imposing proper boundary and initial conditions, see [28], and using the backward Euler method for time discretization, one has to solve a static problem of the form

$$(2.4a) \quad K_i^{-1} \mathbf{v}_i^k + \nabla p_i^k = \mathbf{0}, \quad i = 1, \dots, n,$$

$$(2.4b) \quad -\alpha_i \operatorname{div} \mathbf{u}^k - \tau \operatorname{div} \mathbf{v}_i^k - c_{p_i} p_i^k - \tau \sum_{\substack{j=1 \\ j \neq i}}^n \beta_{ij} (p_i^k - p_j^k) = g_i^k, \quad i = 1, \dots, n,$$

$$(2.4c) \quad -2\mu \operatorname{div} \boldsymbol{\epsilon}(\mathbf{u}^k) - \lambda \nabla \operatorname{div} \mathbf{u}^k + \sum_{i=1}^n \alpha_i \nabla p_i^k = \mathbf{f}^k,$$

in each time step, i.e., at every time moment $t_k = t_{k-1} + \tau$, $k = 1, 2, \dots$. Here, \mathbf{u}^k , \mathbf{v}_i^k , p_i^k are approximations of \mathbf{u} , \mathbf{v}_i , p_i at $t = t_k$ and $\mathbf{f}^k = \mathbf{f}(x, t_k)$, $g_i^k = -\tau g_i(x, t_k) - \alpha_i \operatorname{div}(\mathbf{u}^{k-1}) - c_{p_i} p_i^{k-1}$ for $i = 1, \dots, n$. After dividing (2.4) by 2μ ,

denoting

$$\frac{\lambda}{2\mu} \rightarrow \lambda, \quad \frac{\alpha_i}{2\mu} \rightarrow \alpha_i, \quad \frac{\mathbf{f}^k}{2\mu} \rightarrow \mathbf{f}^k, \quad \frac{\tau}{2\mu} \rightarrow \tau, \quad \frac{c_{p_i}}{2\mu} \rightarrow c_{p_i}, \quad \frac{g_i^k}{2\mu} \rightarrow g_i^k, \quad i = 1, \dots, n,$$

and further introducing the new variables

$$\mathbf{v}_i := \frac{\tau}{\alpha_i} \mathbf{v}_i^k, \quad p_i := \alpha_i p_i^k, \quad \mathbf{u} := \mathbf{u}^k, \quad \mathbf{f} := \mathbf{f}^k, \quad g_i := \frac{g_i^k}{\alpha_i}, \quad i = 1, \dots, n,$$

system (2.4) can be presented in the form

$$(2.5a) \quad \tau^{-1} K_i^{-1} \alpha_i^2 \mathbf{v}_i + \nabla p_i = \mathbf{0}, \quad i = 1, \dots, n,$$

$$(2.5b) \quad -\operatorname{div} \mathbf{u} - \operatorname{div} \mathbf{v}_i - \frac{c_{p_i}}{\alpha_i^2} p_i + \sum_{\substack{j=1 \\ j \neq i}}^n \left(-\frac{\tau \beta_{ij}}{\alpha_i^2} p_i + \frac{\tau \beta_{ij}}{\alpha_i \alpha_j} p_j \right) = g_i, \quad i = 1, \dots, n,$$

$$(2.5c) \quad -\operatorname{div} \epsilon(\mathbf{u}) - \lambda \nabla \operatorname{div} \mathbf{u} + \sum_{i=1}^n \nabla p_i = \mathbf{f},$$

where we have also multiplied (2.4a) by α_i and (2.4b) by α_i^{-1} . In what follows we will also make use of the notation $\mathbf{v}^T := (\mathbf{v}_1^T, \dots, \mathbf{v}_n^T)$, $\mathbf{z}^T := (\mathbf{z}_1^T, \dots, \mathbf{z}_n^T)$, $\mathbf{p}^T := (p_1, \dots, p_n)$, $\mathbf{q}^T := (q_1, \dots, q_n)$ where $\mathbf{v}, \mathbf{z} \in \mathbf{V} = \mathbf{V}_1 \times \dots \times \mathbf{V}_n$, $\mathbf{p}, \mathbf{q} \in \mathbf{P} = P_1 \times \dots \times P_n$ and $\mathbf{U} = \{\mathbf{u} \in H^1(\Omega)^d : \mathbf{u} = \mathbf{0} \text{ on } \Gamma_{\mathbf{u},D}\}$, $\mathbf{V}_i = \{\mathbf{v}_i \in H(\operatorname{div}, \Omega) : \mathbf{v}_i \cdot \mathbf{n} = 0 \text{ on } \Gamma_{p_i,N}\}$, $P_i = L^2(\Omega)$, and $P_i = L_0^2(\Omega)$ if $\Gamma_{\mathbf{u},D} = \Gamma = \partial\Omega$. Using the parameter substitutions

$$R_i^{-1} := \tau^{-1} K_i^{-1} \alpha_i^2, \quad \alpha_{p_i} := \frac{c_{p_i}}{\alpha_i^2}, \quad \beta_{ii} := \sum_{\substack{j=1 \\ j \neq i}}^n \beta_{ij}, \quad \alpha_{ij} := \frac{\tau \beta_{ij}}{\alpha_i \alpha_j}, \quad \tilde{\alpha}_{ii} := -\alpha_{p_i} - \alpha_{ii}$$

for $i, j = 1, \dots, n$, we further rewrite system (2.5) as

$$(2.6) \quad \mathcal{A} \begin{pmatrix} \mathbf{v} \\ \mathbf{p} \\ \mathbf{u} \end{pmatrix} = \begin{bmatrix} A_v & B_v^T & 0 \\ B_v & -C & B_u \\ 0 & B_u^T & A_u \end{bmatrix} \begin{pmatrix} \mathbf{v} \\ \mathbf{p} \\ \mathbf{u} \end{pmatrix} = \begin{pmatrix} \mathbf{0} \\ \mathbf{g} \\ \mathbf{f} \end{pmatrix}$$

where

$$A_v := \begin{bmatrix} R_1^{-1} I & 0 & \dots & 0 \\ 0 & \ddots & & \vdots \\ \vdots & & \ddots & 0 \\ 0 & \dots & 0 & R_n^{-1} I \end{bmatrix}, \quad B_v := \begin{bmatrix} -\operatorname{div} & 0 & \dots & 0 \\ 0 & \ddots & & \vdots \\ \vdots & & \ddots & 0 \\ 0 & \dots & 0 & -\operatorname{div} \end{bmatrix}, \quad B_u := \begin{bmatrix} -\operatorname{div} \\ \vdots \\ \vdots \\ -\operatorname{div} \end{bmatrix}, \quad -C := \begin{bmatrix} \tilde{\alpha}_{11} I & \alpha_{12} I & \dots & \alpha_{1n} I \\ \alpha_{21} I & \ddots & & \alpha_{2n} I \\ \vdots & & \ddots & \vdots \\ \alpha_{n1} I & \alpha_{n2} I & \dots & \tilde{\alpha}_{nn} I \end{bmatrix}$$

and $A_u := -\operatorname{div} \epsilon - \lambda \nabla \operatorname{div}$.

For the scaled parameters, we make the rather non-restrictive assumptions

$$(2.7) \quad \lambda \geq 0, \quad R_1^{-1}, \dots, R_n^{-1} > 0, \quad \alpha_{p_1}, \dots, \alpha_{p_n} \geq 0, \quad \alpha_{ij} \geq 0, \quad i, j = 1, \dots, n.$$

From now on, we will use the same symbols for denoting operators and their corresponding coefficient matrices. Additionally, let us introduce

$$\Lambda_1 := \begin{bmatrix} \alpha_{11} & -\alpha_{12} & \dots & -\alpha_{1n} \\ -\alpha_{21} & \alpha_{22} & \dots & -\alpha_{2n} \\ \vdots & \vdots & \ddots & \vdots \\ -\alpha_{n1} & -\alpha_{n2} & \dots & \alpha_{nn} \end{bmatrix}, \quad \Lambda_2 := \begin{bmatrix} \alpha_{p_1} & 0 & \dots & 0 \\ 0 & \alpha_{p_2} & \dots & 0 \\ \vdots & \vdots & \ddots & \vdots \\ 0 & 0 & \dots & \alpha_{p_n} \end{bmatrix},$$

i.e. $C = \Lambda_1 + \Lambda_2$. Further, denote $R^{-1} := \max\{R_i^{-1} : i = 1, 2, \dots, n\}$, $\lambda_0 := \max\{1, \lambda\}$,

$$\Lambda_3 := \begin{bmatrix} R & 0 & \dots & 0 \\ 0 & \ddots & \ddots & \vdots \\ \vdots & \ddots & \ddots & \vdots \\ 0 & \dots & 0 & R \end{bmatrix}, \quad \Lambda_4 := \begin{bmatrix} \frac{1}{\lambda_0} & \dots & \dots & \frac{1}{\lambda_0} \\ \vdots & & & \vdots \\ \vdots & & & \vdots \\ \frac{1}{\lambda_0} & \dots & \dots & \frac{1}{\lambda_0} \end{bmatrix},$$

$$\Lambda := \Lambda_1 + \Lambda_2 + \Lambda_3 + \Lambda_4,$$

and also, for any block vector \mathbf{z} and vector \mathbf{u}

$$\text{Div} \mathbf{z} := \begin{pmatrix} \text{div} \mathbf{z}_1 \\ \vdots \\ \text{div} \mathbf{z}_n \end{pmatrix}, \quad \underline{\text{Div}} \mathbf{u} := \begin{pmatrix} \text{div} \mathbf{u} \\ \vdots \\ \text{div} \mathbf{u} \end{pmatrix}.$$

2.2. The fixed-stress split iterative method revisited. For any operator $\Lambda_L : \mathbf{P} \rightarrow \mathbf{P}^*$, \mathcal{A} can be decomposed as follows:

$$(2.8) \quad \mathcal{A} = \begin{bmatrix} A_v & B_v^T & 0 \\ B_v & -C - \Lambda_L & 0 \\ 0 & B_u^T & A_u \end{bmatrix} + \begin{bmatrix} 0 & 0 & 0 \\ 0 & \Lambda_L & B_u \\ 0 & 0 & 0 \end{bmatrix}$$

Applying the block Gauss-Seidel method to the above system, we obtain

$$(2.9) \quad \begin{bmatrix} A_v & B_v^T & 0 \\ B_v & -C - \Lambda_L & 0 \\ 0 & B_u^T & A_u \end{bmatrix} \begin{pmatrix} \mathbf{v}^{k+1} \\ \mathbf{p}^{k+1} \\ \mathbf{u}^{k+1} \end{pmatrix} + \begin{bmatrix} 0 & 0 & 0 \\ 0 & \Lambda_L & B_u \\ 0 & 0 & 0 \end{bmatrix} \begin{pmatrix} \mathbf{v}^k \\ \mathbf{p}^k \\ \mathbf{u}^k \end{pmatrix} = \begin{pmatrix} \mathbf{0} \\ \mathbf{g} \\ \mathbf{f} \end{pmatrix}$$

or, equivalently,

$$(2.10) \quad \begin{bmatrix} A_v & B_v^T & 0 \\ B_v & -C - \Lambda_L & 0 \\ 0 & B_u^T & A_u \end{bmatrix} \begin{pmatrix} \mathbf{v}^{k+1} \\ \mathbf{p}^{k+1} \\ \mathbf{u}^{k+1} \end{pmatrix} = \begin{pmatrix} \mathbf{0} \\ \mathbf{g} \\ \mathbf{f} \end{pmatrix} - \begin{bmatrix} 0 & 0 & 0 \\ 0 & \Lambda_L & B_u \\ 0 & 0 & 0 \end{bmatrix} \begin{pmatrix} \mathbf{v}^k \\ \mathbf{p}^k \\ \mathbf{u}^k \end{pmatrix}$$

which is (a block variant of) the fixed-stress method. In [29] a parameter-robust convergence analysis of this method has been presented for the choice

$$(2.11) \quad \Lambda_L = L \begin{bmatrix} I & I & \dots & I \\ I & \ddots & & I \\ \vdots & & \ddots & \vdots \\ I & I & \dots & I \end{bmatrix} \quad \text{where } L \geq \frac{1}{\lambda + c_K^2},$$

and c_K is the constant in the estimate

$$(2.12) \quad \|\epsilon(\mathbf{w})\| \geq c_K \|\text{div} \mathbf{w}\| \quad \text{for all } \mathbf{w} \in \mathbf{U}$$

where $\|\cdot\|$ denotes the L^2 norm, on the left-hand side of (2.12) of a tensor-valued and on the right-hand side of a scalar-valued function. Note that (2.12) holds true for example for $c_K = 1/\sqrt{d}$ where d is the space dimension.

2.3. Uzawa-type methods in block Gauss-Seidel framework. Now for any positive definite operator $M : \mathbf{P}^* \rightarrow \mathbf{P}$, we consider the equivalent augmented MPET system

$$(2.13) \quad \hat{\mathcal{A}} \begin{pmatrix} \mathbf{v} \\ \mathbf{p} \\ \mathbf{u} \end{pmatrix} = \begin{bmatrix} A_v + B_v^T M B_v & B_v^T - B_v^T M C & B_v^T M B_u \\ -B_v & C & -B_u \\ 0 & B_u^T & A_u \end{bmatrix} \begin{pmatrix} \mathbf{v} \\ \mathbf{p} \\ \mathbf{u} \end{pmatrix} = \begin{pmatrix} B_v^T M \mathbf{g} \\ -\mathbf{g} \\ \mathbf{f} \end{pmatrix}.$$

Further, for any positive definite operator $S : \mathbf{P} \rightarrow \mathbf{P}^*$, we decompose $\hat{\mathcal{A}}$ in the form

$$(2.14) \quad \hat{\mathcal{A}} = \begin{bmatrix} A_v + B_v^T M B_v & 0 & 0 \\ -B_v & S & 0 \\ 0 & B_u^T & A_u \end{bmatrix} + \begin{bmatrix} 0 & B_v^T - B_v^T M C & B_v^T M B_u \\ 0 & -S + C & -B_u \\ 0 & 0 & 0 \end{bmatrix}.$$

Next, applying the block Gauss-Seidel method to the above system yields

$$(2.15) \quad \begin{bmatrix} A_v + B_v^T M B_v & 0 & 0 \\ -B_v & S & 0 \\ 0 & B_u^T & A_u \end{bmatrix} \begin{pmatrix} \mathbf{v}^{k+1} \\ \mathbf{p}^{k+1} \\ \mathbf{u}^{k+1} \end{pmatrix} + \begin{bmatrix} 0 & B_v^T - B_v^T M C & B_v^T M B_u \\ 0 & -S + C & -B_u \\ 0 & 0 & 0 \end{bmatrix} \begin{pmatrix} \mathbf{v}^k \\ \mathbf{p}^k \\ \mathbf{u}^k \end{pmatrix} = \begin{pmatrix} B_v^T M \mathbf{g} \\ -\mathbf{g} \\ \mathbf{f} \end{pmatrix},$$

namely

$$(2.16) \quad \begin{bmatrix} A_v + B_v^T M B_v & 0 & 0 \\ -B_v & S & 0 \\ 0 & B_u^T & A_u \end{bmatrix} \begin{pmatrix} \mathbf{v}^{k+1} \\ \mathbf{p}^{k+1} \\ \mathbf{u}^{k+1} \end{pmatrix} = \begin{pmatrix} B_v^T M \mathbf{g} \\ -\mathbf{g} \\ \mathbf{f} \end{pmatrix} - \begin{bmatrix} 0 & B_v^T - B_v^T M C & B_v^T M B_u \\ 0 & -S + C & -B_u \\ 0 & 0 & 0 \end{bmatrix} \begin{pmatrix} \mathbf{v}^k \\ \mathbf{p}^k \\ \mathbf{u}^k \end{pmatrix}.$$

System (2.16) can be expressed in terms of bilinear forms as follows:

Algorithm 1 Fully decoupled iterative scheme for weak flux-pressure-displacement formulation of MPET problem

Step a: Given \mathbf{p}^k and \mathbf{u}^k , we first solve for \mathbf{v}^{k+1} , such that for all $\mathbf{z} \in \mathbf{V}$ there holds

$$(2.17) \quad (A_v \mathbf{v}^{k+1}, \mathbf{z}) + (M \text{Div} \mathbf{v}^{k+1}, \text{Div} \mathbf{z}) = -(M \mathbf{g}, \text{Div} \mathbf{z}) + (\mathbf{p}^k, \text{Div} \mathbf{z}) - (M(\Lambda_1 + \Lambda_2) \mathbf{p}^k, \text{Div} \mathbf{z}) - (M \text{Div} \mathbf{u}^k, \text{Div} \mathbf{z}).$$

Step b: Given \mathbf{u}^k and \mathbf{v}^{k+1} , we solve for \mathbf{p}^{k+1} , such that for all $\mathbf{q} \in \mathbf{P}$ there holds

$$(2.18) \quad (S \mathbf{p}^{k+1}, \mathbf{q}) = -(\mathbf{g}, \mathbf{q}) + (S \mathbf{p}^k, \mathbf{q}) - ((\Lambda_1 + \Lambda_2) \mathbf{p}^k, \mathbf{q}) - (\text{Div} \mathbf{u}^k, \mathbf{q}) - (\text{Div} \mathbf{v}^{k+1}, \mathbf{q}).$$

Step c: Given \mathbf{p}^{k+1} and \mathbf{v}^{k+1} , we solve for \mathbf{u}^{k+1} , such that for all $\mathbf{w} \in \mathbf{U}$ there holds

$$(2.19) \quad (\epsilon(\mathbf{u}^{k+1}), \epsilon(\mathbf{w})) + \lambda(\text{div} \mathbf{u}^{k+1}, \text{div} \mathbf{w}) = (\mathbf{f}, \mathbf{w}) + (\mathbf{p}^{k+1}, \text{Div} \mathbf{w}).$$

2.4. Preliminary results. We first present a result from linear algebra which will be useful in the proof of Theorem 3.4 in Section 3.

Lemma 2.1. For any $a > 0$ and $b > 0$, denote $\mathbf{e} = \underbrace{(1, \dots, 1)}_n^T$ and $(aI_{n \times n} + b\mathbf{e}\mathbf{e}^T)^{-1} = (b_{ij})_{n \times n}$. Then we have that

$$(2.20) \quad 0 < \sum_{i=1}^n \sum_{j=1}^n b_{ij} = \frac{n}{(a + nb)}.$$

Proof. The proof is based on the Sherman-Morrison-Woodbury formula and follows the arguments of the proof of Lemma 1 in [28]. \square

Next, let us recall some well known results, see [18, 15].

Lemma 2.2. *There exists a constant $\beta_s > 0$ such that:*

$$(2.21) \quad \inf_{(q_1, \dots, q_n) \in P_1 \times \dots \times P_n} \sup_{\mathbf{u} \in \mathbf{U}} \frac{(\operatorname{div} \mathbf{u}, \sum_{i=1}^n q_i)}{\|\mathbf{u}\|_1 \left\| \sum_{i=1}^n q_i \right\|} \geq \beta_s$$

Lemma 2.3. *There exists a constant $\beta_d > 0$ such that:*

$$(2.22) \quad \inf_{q \in P_i} \sup_{\mathbf{v} \in \mathbf{V}_i} \frac{(\operatorname{div} \mathbf{v}, q)}{\|\mathbf{v}\|_{\operatorname{div}} \|q\|} \geq \beta_d, \quad i = 1, \dots, n.$$

Here $\|\cdot\|_1$ and $\|\mathbf{v}\|_{\operatorname{div}}$ denote the standard H^1 and $H(\operatorname{div})$ norms of vector-valued functions, respectively, i.e., $\|\mathbf{u}\|_1^2 := \int_{\Omega} \nabla \mathbf{u} : \nabla \mathbf{u} + \mathbf{u} \cdot \mathbf{u} \, dx$ and $\|\mathbf{v}\|_{\operatorname{div}}^2 := \int_{\Omega} \operatorname{div} \mathbf{v} \operatorname{div} \mathbf{v} + \mathbf{v} \cdot \mathbf{v} \, dx$.

Our task will be to study the errors

$$(2.23a) \quad \mathbf{e}_u^k = \mathbf{u}^k - \mathbf{u} \in \mathbf{U},$$

$$(2.23b) \quad \mathbf{e}_{v_i}^k = \mathbf{v}_i^k - \mathbf{v}_i \in \mathbf{V}_i, \quad i = 1, \dots, n,$$

$$(2.23c) \quad e_{p_i}^k = p_i^k - p_i \in P_i, \quad i = 1, \dots, n,$$

of the k -th iterates \mathbf{u}^k , \mathbf{v}_i^k , p_i^k , $i = 1, \dots, n$, generated by Algorithm 1. For that reason, we consider the following error equations

$$(2.24a) \quad (A_v \mathbf{e}_v^{k+1}, \mathbf{z}) - (\mathbf{e}_p^k, \operatorname{Div} \mathbf{z}) + (M \operatorname{Div} \mathbf{e}_u^k, \operatorname{Div} \mathbf{z}) + (M \operatorname{Div} \mathbf{e}_v^{k+1}, \operatorname{Div} \mathbf{z}) + (M(\Lambda_1 + \Lambda_2) \mathbf{e}_p^k, \operatorname{Div} \mathbf{z}) = 0,$$

$$(2.24b) \quad (S \mathbf{e}_p^{k+1}, \mathbf{q}) - (S \mathbf{e}_p^k, \mathbf{q}) + (\operatorname{Div} \mathbf{e}_u^k, \mathbf{q}) + (\operatorname{Div} \mathbf{e}_v^{k+1}, \mathbf{q}) + ((\Lambda_1 + \Lambda_2) \mathbf{e}_p^k, \mathbf{q}) = 0,$$

$$(2.24c) \quad (\epsilon(\mathbf{e}_u^{k+1}), \epsilon(\mathbf{w})) + \lambda(\operatorname{div} \mathbf{e}_u^{k+1}, \operatorname{div} \mathbf{w}) - (\mathbf{e}_p^{k+1}, \operatorname{Div} \mathbf{w}) = 0$$

where the error block-vectors \mathbf{e}_v^k and \mathbf{e}_p^k are given by $(\mathbf{e}_v^k)^T = ((e_{v_1}^k)^T, \dots, (e_{v_n}^k)^T)^T$, $(\mathbf{e}_p^k)^T = (e_{p_1}^k, \dots, e_{p_n}^k)$.

To complete the design of Algorithm 1, we need to specify M and S . By Lemma 2.3 we have that for all $\mathbf{e}_{p_i}^{k+1} \in P_i$ there exists $\psi_i \in \mathbf{V}_i$ such that $\operatorname{div} \psi_i = \mathbf{e}_{p_i}^{k+1}$ and $\|\psi_i\|_{\operatorname{div}} \leq \beta_d^{-1} \|\mathbf{e}_{p_i}^{k+1}\|$ for all $i = 1, \dots, n$, i.e., $\operatorname{Div} \psi = \mathbf{e}_p^{k+1}$ and $\|\psi\|_{\operatorname{div}} \leq \beta_v^{-1} \|\mathbf{e}_p^{k+1}\|$. Setting $\mathbf{q} = S^{-1} \mathbf{e}_p^{k+1}$ in (2.24b) and $\mathbf{z} = \psi$ in (2.24a), from $\operatorname{Div} \psi = \mathbf{e}_p^{k+1}$ it follows that

$$(2.25a) \quad (A_v \mathbf{e}_v^{k+1}, \psi) - (\mathbf{e}_p^k, \mathbf{e}_p^{k+1}) + (M \operatorname{Div} \mathbf{e}_u^{k+1}, \mathbf{e}_p^{k+1}) + (M \operatorname{Div} \mathbf{e}_v^{k+1}, \mathbf{e}_p^{k+1}) + (M(\Lambda_1 + \Lambda_2) \mathbf{e}_p^k, \mathbf{e}_p^{k+1}) = 0,$$

$$(2.25b) \quad (\mathbf{e}_p^{k+1}, \mathbf{e}_p^{k+1}) - (\mathbf{e}_p^k, \mathbf{e}_p^{k+1}) + (S^{-1} \operatorname{Div} \mathbf{e}_u^k, \mathbf{e}_p^{k+1}) + (S^{-1} \operatorname{Div} \mathbf{e}_v^{k+1}, \mathbf{e}_p^{k+1}) + (S^{-1}(\Lambda_1 + \Lambda_2) \mathbf{e}_p^k, \mathbf{e}_p^{k+1}) = 0.$$

Subtracting (2.25a) from (2.25b) yields

$$\|\mathbf{e}_p^{k+1}\|^2 = (A_v \mathbf{e}_v^{k+1}, \psi) - ((S^{-1} - M)(\operatorname{Div} \mathbf{e}_u^k + \operatorname{Div} \mathbf{e}_v^{k+1} + (\Lambda_1 + \Lambda_2) \mathbf{e}_p^k), \mathbf{e}_p^{k+1}),$$

implying

$$\begin{aligned} \|\mathbf{e}_p^{k+1}\|^2 &\leq \|A_v^{\frac{1}{2}} \mathbf{e}_v^{k+1}\| \|A_v^{\frac{1}{2}} \psi\| + \|(S^{-1} - M)(\operatorname{Div} \mathbf{e}_u^k + \operatorname{Div} \mathbf{e}_v^{k+1} + (\Lambda_1 + \Lambda_2) \mathbf{e}_p^k)\| \|\mathbf{e}_p^{k+1}\| \\ &\leq \sqrt{R^{-1}} \|A_v^{\frac{1}{2}} \mathbf{e}_v^{k+1}\| \|\psi\| + \|(S^{-1} - M)(\operatorname{Div} \mathbf{e}_u^k + \operatorname{Div} \mathbf{e}_v^{k+1} + (\Lambda_1 + \Lambda_2) \mathbf{e}_p^k)\| \|\mathbf{e}_p^{k+1}\| \\ &\leq \beta_d^{-1} \sqrt{R^{-1}} \|A_v^{\frac{1}{2}} \mathbf{e}_v^{k+1}\| \|\mathbf{e}_p^{k+1}\| + \|(S^{-1} - M)(\operatorname{Div} \mathbf{e}_u^k + \operatorname{Div} \mathbf{e}_v^{k+1} + (\Lambda_1 + \Lambda_2) \mathbf{e}_p^k)\| \|\mathbf{e}_p^{k+1}\|. \end{aligned}$$

We conclude that

$$(2.26) \quad \|\mathbf{e}_p^{k+1}\| \leq \beta_d^{-1} \sqrt{R^{-1}} \|A_v^{\frac{1}{2}} \mathbf{e}_v^{k+1}\| + \|(S^{-1} - M)(\operatorname{Div} \mathbf{e}_u^k + \operatorname{Div} \mathbf{e}_v^{k+1} + (\Lambda_1 + \Lambda_2) \mathbf{e}_p^k)\|.$$

Estimate (2.26) suggests choosing $S = M^{-1}$ in order to minimize the upper bound for $\|\mathbf{e}_p^{k+1}\|$. This results in the following statement.

Lemma 2.4. *Consider Algorithm 1 and let $S = M^{-1}$, then we have*

$$(2.27) \quad \|A_v^{\frac{1}{2}} \mathbf{e}_v^{k+1}\|^2 \geq R\beta_d^2 \|\mathbf{e}_p^{k+1}\|^2 = \beta_d^2 \|\Lambda_3^{\frac{1}{2}} \mathbf{e}_p^{k+1}\|^2.$$

The relationship $S = M^{-1}$ reduces our design task to the determination of either S or M . In the remainder of this paper, we analyze and numerically test Algorithm 1 for the specific choice

$$(2.28) \quad S := \Lambda_1 + \Lambda_2 + L_1 \Lambda_3 + L_2 \Lambda_4,$$

where L_1 and L_2 are scalar parameters which are later to be determined.

3. CONVERGENCE THEORY OF UZAWA-TYPE ALGORITHMS FOR MPET

This section is devoted to the convergence analysis of Algorithm 1. Our aim is to establish a uniform bound on the convergence rate, i.e., a bound independent of any model and discretization parameters.

We start with deriving some useful auxiliary results presented in the following two lemmas. These afterwards assist us in establishing a parameter-robust upper bound on the pressure error in a weighted norm.

Lemma 3.1. *Considering Algorithm 1 with S as defined in (2.28), the errors \mathbf{e}_u^k , \mathbf{e}_v^k and \mathbf{e}_p^k defined in (2.23) satisfy the following estimate:*

$$(3.1) \quad \begin{aligned} & \frac{1}{2} \|\epsilon(\mathbf{e}_u^{k+1})\|^2 + \frac{\lambda}{2} \|\text{div} \mathbf{e}_u^{k+1}\|^2 + \|A_v^{\frac{1}{2}} \mathbf{e}_v^{k+1}\|^2 + \|(\Lambda_1 + \Lambda_2)^{\frac{1}{2}} \mathbf{e}_p^{k+1}\|^2 + \frac{L_1}{2} \|\Lambda_3^{\frac{1}{2}} \mathbf{e}_p^{k+1}\|^2 + \frac{L_2}{2} \|\Lambda_4^{\frac{1}{2}} \mathbf{e}_p^{k+1}\|^2 \\ & \leq \frac{L_1}{2} \|\Lambda_3^{\frac{1}{2}} \mathbf{e}_p^k\|^2 + \frac{L_2}{2} \|\Lambda_4^{\frac{1}{2}} \mathbf{e}_p^k\|^2 + \left(\frac{\lambda_0}{2(c_K^2 + \lambda)} - \frac{L_2}{2} - \frac{L_1 R \lambda_0}{2n} \right) \|\Lambda_4^{\frac{1}{2}} (\mathbf{e}_p^{k+1} - \mathbf{e}_p^k)\|^2. \end{aligned}$$

Proof. By setting $\mathbf{q} = M \text{Div} \mathbf{e}_v^{k+1}$ in (2.24b) and $\mathbf{z} = \mathbf{e}_v^{k+1}$ in (2.24a) we obtain

$$\begin{aligned} (A_v \mathbf{e}_v^{k+1}, \mathbf{e}_v^{k+1}) - (\mathbf{e}_p^k, \text{Div} \mathbf{e}_v^{k+1}) + (M \underline{\text{Div}} \mathbf{e}_u^k, \text{Div} \mathbf{e}_v^{k+1}) + (M \text{Div} \mathbf{e}_v^{k+1}, \text{Div} \mathbf{e}_v^{k+1}) + (M(\Lambda_1 + \Lambda_2) \mathbf{e}_p^k, \text{Div} \mathbf{e}_v^{k+1}) &= 0, \\ (\mathbf{e}_p^{k+1}, \text{Div} \mathbf{e}_v^{k+1}) = (\mathbf{e}_p^k, \text{Div} \mathbf{e}_v^{k+1}) - (M \underline{\text{Div}} \mathbf{e}_u^k, \text{Div} \mathbf{e}_v^{k+1}) - (M \text{Div} \mathbf{e}_v^{k+1}, \text{Div} \mathbf{e}_v^{k+1}) - (M(\Lambda_1 + \Lambda_2) \mathbf{e}_p^k, \text{Div} \mathbf{e}_v^{k+1}) \end{aligned}$$

from where it immediately follows that

$$(3.2) \quad (\mathbf{e}_p^{k+1}, \text{Div} \mathbf{e}_v^{k+1}) = (A_v \mathbf{e}_v^{k+1}, \mathbf{e}_v^{k+1}).$$

Choosing $\mathbf{q} = \mathbf{e}_p^{k+1}$ in (2.24b) and $\mathbf{w} = \mathbf{e}_u^{k+1}$ in (2.24c) yields

$$(3.3a) \quad (\epsilon(\mathbf{e}_u^{k+1}), \epsilon(\mathbf{e}_u^{k+1})) + \lambda(\text{div} \mathbf{e}_u^{k+1}, \text{div} \mathbf{e}_u^{k+1}) - (\mathbf{e}_p^{k+1}, \underline{\text{Div}} \mathbf{e}_u^{k+1}) = 0,$$

$$(3.3b) \quad (S \mathbf{e}_p^{k+1}, \mathbf{e}_p^{k+1}) = (S \mathbf{e}_p^k, \mathbf{e}_p^{k+1}) - (\underline{\text{Div}} \mathbf{e}_u^k, \mathbf{e}_p^{k+1}) - (\text{Div} \mathbf{e}_v^{k+1}, \mathbf{e}_p^{k+1}) - ((\Lambda_1 + \Lambda_2) \mathbf{e}_p^k, \mathbf{e}_p^{k+1}).$$

Next, summing (3.3a) and (3.3b) and applying (3.2) it follows that

$$(3.4) \quad \|\epsilon(\mathbf{e}_u^{k+1})\|^2 + \lambda \|\text{div} \mathbf{e}_u^{k+1}\|^2 + \|S^{\frac{1}{2}} \mathbf{e}_p^{k+1}\|^2 - ((L_1 \Lambda_3 + L_2 \Lambda_4) \mathbf{e}_p^k, \mathbf{e}_p^{k+1}) = (\text{Div} \mathbf{e}_u^{k+1} - \underline{\text{Div}} \mathbf{e}_u^k, \mathbf{e}_p^{k+1}) - \|A_v^{\frac{1}{2}} \mathbf{e}_v^{k+1}\|^2.$$

In order to simplify (3.4) we first rewrite $\|S^{\frac{1}{2}}\mathbf{e}_p^{k+1}\|^2 - ((L_1\Lambda_3 + L_2\Lambda_4)\mathbf{e}_p^k, \mathbf{e}_p^{k+1})$, that is,

$$\begin{aligned}
\|S^{\frac{1}{2}}\mathbf{e}_p^{k+1}\|^2 - ((L_1\Lambda_3 + L_2\Lambda_4)\mathbf{e}_p^k, \mathbf{e}_p^{k+1}) &= \|(\Lambda_1 + \Lambda_2)^{\frac{1}{2}}\mathbf{e}_p^{k+1}\|^2 + \frac{L_1}{2}(\|\Lambda_3^{\frac{1}{2}}\mathbf{e}_p^{k+1}\|^2 - \|\Lambda_3^{\frac{1}{2}}\mathbf{e}_p^k\|^2 + \|\Lambda_3^{\frac{1}{2}}(\mathbf{e}_p^{k+1} - \mathbf{e}_p^k)\|^2) \\
&\quad + \frac{L_2}{2}\left(\|\Lambda_4^{\frac{1}{2}}\mathbf{e}_p^{k+1}\|^2 - \|\Lambda_4^{\frac{1}{2}}\mathbf{e}_p^k\|^2 + \|\Lambda_4^{\frac{1}{2}}(\mathbf{e}_p^{k+1} - \mathbf{e}_p^k)\|^2\right) \\
&\geq \|(\Lambda_1 + \Lambda_2)^{\frac{1}{2}}\mathbf{e}_p^{k+1}\|^2 + \frac{L_1}{2}\|\Lambda_3^{\frac{1}{2}}\mathbf{e}_p^{k+1}\|^2 + \frac{L_2}{2}\|\Lambda_4^{\frac{1}{2}}\mathbf{e}_p^{k+1}\|^2 \\
&\quad - \frac{L_1}{2}\|\Lambda_3^{\frac{1}{2}}\mathbf{e}_p^k\|^2 - \frac{L_2}{2}\|\Lambda_4^{\frac{1}{2}}\mathbf{e}_p^k\|^2 + \left(\frac{L_2}{2} + \frac{L_1 R \lambda_0}{2n}\right)\|\Lambda_4^{\frac{1}{2}}(\mathbf{e}_p^{k+1} - \mathbf{e}_p^k)\|^2.
\end{aligned} \tag{3.5}$$

Second, we estimate $(\underline{\text{Div}}\mathbf{e}_u^{k+1} - \underline{\text{Div}}\mathbf{e}_u^k, \mathbf{e}_p^{k+1})$. By setting $\mathbf{w} = \mathbf{e}_u^{k+1} - \mathbf{e}_u^k$ in (2.24c) we obtain

$$\begin{aligned}
(\mathbf{e}_p^{k+1}, \underline{\text{Div}}(\mathbf{e}_u^{k+1} - \mathbf{e}_u^k)) &= (\epsilon(\mathbf{e}_u^{k+1} - \mathbf{e}_u^k), \epsilon(\mathbf{e}_u^{k+1})) + \lambda(\text{div}(\mathbf{e}_u^{k+1} - \mathbf{e}_u^k), \text{div}\mathbf{e}_u^{k+1}) \\
&\leq \frac{1}{2}(\|\epsilon(\mathbf{e}_u^{k+1} - \mathbf{e}_u^k)\|^2 + \lambda\|\text{div}(\mathbf{e}_u^{k+1} - \mathbf{e}_u^k)\|^2) + \frac{1}{2}(\|\epsilon(\mathbf{e}_u^{k+1})\|^2 + \lambda\|\text{div}\mathbf{e}_u^{k+1}\|^2).
\end{aligned} \tag{3.6}$$

In order to estimate the right-hand side of (3.6), we subtract the k -th error from the $(k+1)$ -th error and choose $\mathbf{w} = \mathbf{e}_u^{k+1} - \mathbf{e}_u^k$ in (2.24c) and herewith obtaining

$$\|\epsilon(\mathbf{e}_u^{k+1} - \mathbf{e}_u^k)\|^2 + \lambda\|\text{div}(\mathbf{e}_u^{k+1} - \mathbf{e}_u^k)\|^2 = \left(\sum_{i=1}^n (\mathbf{e}_{p_i}^{k+1} - \mathbf{e}_{p_i}^k), \text{div}(\mathbf{e}_u^{k+1} - \mathbf{e}_u^k)\right).$$

Applying Cauchy's inequality further yields

$$\begin{aligned}
\|\epsilon(\mathbf{e}_u^{k+1} - \mathbf{e}_u^k)\|^2 + \lambda\|\text{div}(\mathbf{e}_u^{k+1} - \mathbf{e}_u^k)\|^2 &= \left(\sum_{i=1}^n (\mathbf{e}_{p_i}^{k+1} - \mathbf{e}_{p_i}^k), \text{div}(\mathbf{e}_u^{k+1} - \mathbf{e}_u^k)\right) \leq \left\|\sum_{i=1}^n (\mathbf{e}_{p_i}^{k+1} - \mathbf{e}_{p_i}^k)\right\| \cdot \|\text{div}(\mathbf{e}_u^{k+1} - \mathbf{e}_u^k)\| \\
&= \sqrt{\lambda_0}\|\Lambda_4^{\frac{1}{2}}(\mathbf{e}_p^{k+1} - \mathbf{e}_p^k)\| \cdot \|\text{div}(\mathbf{e}_u^{k+1} - \mathbf{e}_u^k)\|.
\end{aligned} \tag{3.7}$$

Noting that

$$(c_K^2 + \lambda)\|\text{div}\mathbf{w}\|^2 \leq \|\epsilon(\mathbf{w})\|^2 + \lambda\|\text{div}\mathbf{w}\|^2, \tag{3.8}$$

which follows from (2.12), we directly obtain

$$(c_K^2 + \lambda)\|\text{div}(\mathbf{e}_u^{k+1} - \mathbf{e}_u^k)\|^2 \leq \sqrt{\lambda_0}\|\Lambda_4^{\frac{1}{2}}(\mathbf{e}_p^{k+1} - \mathbf{e}_p^k)\| \cdot \|\text{div}(\mathbf{e}_u^{k+1} - \mathbf{e}_u^k)\|,$$

from (3.7). The latter estimate implies

$$\|\text{div}(\mathbf{e}_u^{k+1} - \mathbf{e}_u^k)\| \leq \frac{\sqrt{\lambda_0}}{c_K^2 + \lambda}\|\Lambda_4^{\frac{1}{2}}(\mathbf{e}_p^{k+1} - \mathbf{e}_p^k)\|.$$

By using the above inequality in (3.7), it follows that

$$\|\epsilon(\mathbf{e}_u^{k+1} - \mathbf{e}_u^k)\|^2 + \lambda\|\text{div}(\mathbf{e}_u^{k+1} - \mathbf{e}_u^k)\|^2 \leq \frac{\lambda_0}{c_K^2 + \lambda}\|\Lambda_4^{\frac{1}{2}}(\mathbf{e}_p^{k+1} - \mathbf{e}_p^k)\|^2. \tag{3.9}$$

Now, combining (3.6) and (3.9) yields

$$(\mathbf{e}_p^{k+1}, \underline{\text{Div}}(\mathbf{e}_u^{k+1} - \mathbf{e}_u^k)) \leq \frac{\lambda_0}{2(c_K^2 + \lambda)}\|\Lambda_4^{\frac{1}{2}}(\mathbf{e}_p^{k+1} - \mathbf{e}_p^k)\|^2 + \frac{1}{2}(\|\epsilon(\mathbf{e}_u^{k+1})\|^2 + \lambda\|\text{div}\mathbf{e}_u^{k+1}\|^2). \tag{3.10}$$

Finally, inserting (3.5) and (3.10) in (3.4) we have that

$$\begin{aligned} & \|\epsilon(\mathbf{e}_u^{k+1})\|^2 + \lambda \|\operatorname{div} \mathbf{e}_u^{k+1}\|^2 + \|(\Lambda_1 + \Lambda_2)^{\frac{1}{2}} \mathbf{e}_p^{k+1}\|^2 + \frac{L_1}{2} \|\Lambda_3^{\frac{1}{2}} \mathbf{e}_p^{k+1}\|^2 + \frac{L_2}{2} \|\Lambda_4^{\frac{1}{2}} \mathbf{e}_p^{k+1}\|^2 \\ & \leq \frac{\lambda_0}{2(c_K^2 + \lambda)} \|\Lambda_4^{\frac{1}{2}} (\mathbf{e}_p^{k+1} - \mathbf{e}_p^k)\|^2 + \frac{1}{2} (\|\epsilon(\mathbf{e}_u^{k+1})\|^2 + \lambda \|\operatorname{div} \mathbf{e}_u^{k+1}\|^2) - \|\Lambda_v^{\frac{1}{2}} \mathbf{e}_v^{k+1}\|^2 \\ & \quad + \frac{L_1}{2} \|\Lambda_3^{\frac{1}{2}} \mathbf{e}_p^k\|^2 + \frac{L_2}{2} \|\Lambda_4^{\frac{1}{2}} \mathbf{e}_p^k\|^2 - \left(\frac{L_2}{2} + \frac{L_1 R \lambda_0}{2n} \right) \|\Lambda_4^{\frac{1}{2}} (\mathbf{e}_p^{k+1} - \mathbf{e}_p^k)\|^2 \end{aligned}$$

which shows (3.1). \square

The next lemma provides a preliminary estimate for the pressure errors.

Lemma 3.2. *Consider Algorithm 1 with S as in (2.28). Then the errors \mathbf{e}_p^k defined in (2.23) satisfy*

$$\begin{aligned} & \frac{\lambda_0}{2(\beta_s^{-2} + \lambda)} \|\Lambda_4^{\frac{1}{2}} \mathbf{e}_p^{k+1}\|^2 + \beta_d^2 \|\Lambda_3^{\frac{1}{2}} \mathbf{e}_p^{k+1}\|^2 + \|(\Lambda_1 + \Lambda_2)^{\frac{1}{2}} \mathbf{e}_p^{k+1}\|^2 + \frac{L_1}{2} \|\Lambda_3^{\frac{1}{2}} \mathbf{e}_p^{k+1}\|^2 + \frac{L_2}{2} \|\Lambda_4^{\frac{1}{2}} \mathbf{e}_p^{k+1}\|^2 \\ & \leq \frac{L_1}{2} \|\Lambda_3^{\frac{1}{2}} \mathbf{e}_p^k\|^2 + \frac{L_2}{2} \|\Lambda_4^{\frac{1}{2}} \mathbf{e}_p^k\|^2 + \left(\frac{\lambda_0}{2(c_K^2 + \lambda)} - \frac{L_2}{2} - \frac{L_1 R \lambda_0}{2n} \right) \|\Lambda_4^{\frac{1}{2}} (\mathbf{e}_p^{k+1} - \mathbf{e}_p^k)\|^2. \end{aligned}$$

Proof. From Lemma 2.2, it follows that for all $\sum_{i=1}^n \mathbf{e}_{p_i}^{k+1} \in P_i$ there exists $\mathbf{w}_0 \in \mathbf{U}$ such that $\operatorname{div} \mathbf{w}_0 = \frac{1}{\sqrt{\lambda_0}} \sum_{i=1}^n \mathbf{e}_{p_i}^{k+1}$ and $\|\mathbf{w}_0\|_1 \leq \beta_s^{-1} \frac{1}{\sqrt{\lambda_0}} \|\sum_{i=1}^n \mathbf{e}_{p_i}^{k+1}\| = \beta_s^{-1} \|\Lambda_4^{\frac{1}{2}} \mathbf{e}_p^{k+1}\|$. Also,

$$\operatorname{Div} \mathbf{w}_0 = \begin{pmatrix} \frac{1}{\sqrt{\lambda_0}} \sum_{i=1}^n \mathbf{e}_{p_i}^{k+1} \\ \vdots \\ \frac{1}{\sqrt{\lambda_0}} \sum_{i=1}^n \mathbf{e}_{p_i}^{k+1} \end{pmatrix} = \sqrt{\lambda_0} \Lambda_4 \mathbf{e}_p^{k+1}.$$

Setting $\mathbf{w} = \mathbf{w}_0$ in (2.24c), it follows that

$$\begin{aligned} \sqrt{\lambda_0} \|\Lambda_4^{\frac{1}{2}} \mathbf{e}_p^{k+1}\|^2 &= (\epsilon(\mathbf{e}_u^{k+1}), \epsilon(\mathbf{w}_0)) + \lambda (\operatorname{div} \mathbf{e}_u^{k+1}, \operatorname{div} \mathbf{w}_0) \leq (\|\epsilon(\mathbf{e}_u^{k+1})\|^2 + \lambda \|\operatorname{div} \mathbf{e}_u^{k+1}\|^2)^{\frac{1}{2}} \cdot (\|\epsilon(\mathbf{w}_0)\|^2 + \lambda \|\operatorname{div} \mathbf{w}_0\|^2)^{\frac{1}{2}} \\ &\leq (\|\epsilon(\mathbf{e}_u^{k+1})\|^2 + \lambda \|\operatorname{div} \mathbf{e}_u^{k+1}\|^2)^{\frac{1}{2}} \cdot (\beta_s^{-2} \|\Lambda_4^{\frac{1}{2}} \mathbf{e}_p^{k+1}\|^2 + \lambda \|\Lambda_4^{\frac{1}{2}} \mathbf{e}_p^{k+1}\|^2)^{\frac{1}{2}} \\ &= (\|\epsilon(\mathbf{e}_u^{k+1})\|^2 + \lambda \|\operatorname{div} \mathbf{e}_u^{k+1}\|^2)^{\frac{1}{2}} \cdot (\beta_s^{-2} + \lambda)^{\frac{1}{2}} \|\Lambda_4^{\frac{1}{2}} \mathbf{e}_p^{k+1}\| \end{aligned}$$

and, therefore,

$$(3.11) \quad \frac{\lambda_0}{\beta_s^{-2} + \lambda} \|\Lambda_4^{\frac{1}{2}} \mathbf{e}_p^{k+1}\|^2 \leq \|\epsilon(\mathbf{e}_u^{k+1})\|^2 + \lambda \|\operatorname{div} \mathbf{e}_u^{k+1}\|^2.$$

Using (3.11) and (2.27) in (3.1), we have

$$\begin{aligned} & \frac{\lambda_0}{2(\beta_s^{-2} + \lambda)} \|\Lambda_4^{\frac{1}{2}} \mathbf{e}_p^{k+1}\|^2 + \beta_d^2 \|\Lambda_3^{\frac{1}{2}} \mathbf{e}_p^{k+1}\|^2 + \|(\Lambda_1 + \Lambda_2)^{\frac{1}{2}} \mathbf{e}_p^{k+1}\|^2 + \frac{L_1}{2} \|\Lambda_3^{\frac{1}{2}} \mathbf{e}_p^{k+1}\|^2 + \frac{L_2}{2} \|\Lambda_4^{\frac{1}{2}} \mathbf{e}_p^{k+1}\|^2 \\ (3.12) \quad & \leq \frac{L_1}{2} \|\Lambda_3^{\frac{1}{2}} \mathbf{e}_p^k\|^2 + \frac{L_2}{2} \|\Lambda_4^{\frac{1}{2}} \mathbf{e}_p^k\|^2 + \left(\frac{\lambda_0}{2(c_K^2 + \lambda)} - \frac{L_2}{2} - \frac{L_1 R \lambda_0}{2n} \right) \|\Lambda_4^{\frac{1}{2}} (\mathbf{e}_p^{k+1} - \mathbf{e}_p^k)\|^2. \end{aligned}$$

\square

The following two theorems present the main convergence results for Algorithm 1.

Theorem 3.3. Consider Algorithm 1. For any $\theta > 0$ and $L_2 \geq \frac{\lambda_0}{(c_K^2 + \lambda) \left(1 + \frac{\theta \beta_d^2 R \lambda_0}{n}\right)}$, $L_1 = \theta \beta_d^2 L_2$, the errors $\mathbf{e}_{\mathbf{p}}^k$ defined in (2.23) satisfy the estimate:

$$(3.13) \quad \|\mathbf{e}_{\mathbf{p}}^{k+1}\|_{\mathbf{P}_{\theta}}^2 \leq \text{rate}^2(\lambda, R, \theta) \|\mathbf{e}_{\mathbf{p}}^k\|_{\mathbf{P}_{\theta}}^2$$

with

$$\text{rate}^2(\lambda, R, \theta) \leq \frac{1}{C+1}, \quad C = \min \left\{ \frac{\lambda_0}{\beta_s^{-2} + \lambda}, 2\theta^{-1} \right\} L_2^{-1}$$

and

$$(3.14) \quad \|\mathbf{e}_{\mathbf{p}}^{k+1}\|_{\mathbf{P}_{\theta}}^2 := \|\Lambda_4^{\frac{1}{2}} \mathbf{e}_{\mathbf{p}}^{k+1}\|^2 + \theta \beta_d^2 \|\Lambda_3^{\frac{1}{2}} \mathbf{e}_{\mathbf{p}}^{k+1}\|^2 + \|(\Lambda_1 + \Lambda_2)^{\frac{1}{2}} \mathbf{e}_{\mathbf{p}}^{k+1}\|^2.$$

(1) For $\theta = \theta_0 := \beta_d^{-2}$ and $L_2 = \frac{\lambda_0}{(c_K^2 + \lambda) \left(1 + \frac{R \lambda_0}{n}\right)}$, we obtain the convergence factor under the norm $\|\cdot\|_{\mathbf{P}_{\theta_0}}$ estimated by

$$\text{rate}^2(\lambda, R) \leq \frac{1}{\frac{c_0(c_K^2 + \lambda) \left(1 + \frac{\lambda_0 R}{n}\right)}{\lambda_0} + 1} \leq \max \left\{ \frac{1}{c_0 + 1}, \frac{1}{c_0 c_K^2 + 1}, \frac{1}{2} \right\}, \text{ where } c_0 = \min \left\{ \frac{\lambda_0}{\beta_s^{-2} + \lambda}, 2\beta_d^2 \right\}.$$

Here for any $\mathbf{x} \in \mathbf{P}$

$$\|\mathbf{x}\|_{\mathbf{P}_{\theta_0}}^2 := \|\Lambda_3^{\frac{1}{2}} \mathbf{x}\|^2 + \|\Lambda_4^{\frac{1}{2}} \mathbf{x}\|^2 + \|(\Lambda_1 + \Lambda_2)^{\frac{1}{2}} \mathbf{x}\|^2.$$

(2) For the best choice $\theta = \theta_* := \frac{2(\beta_s^{-2} + \lambda)}{\lambda_0}$ and $L_2 = \frac{\lambda_0}{(c_K^2 + \lambda) \left(1 + \frac{2\beta_d^2(\beta_s^{-2} + \lambda)R}{n}\right)}$, the errors $\mathbf{e}_{\mathbf{p}}^k$ satisfy the estimate

$$(3.15) \quad \|\mathbf{e}_{\mathbf{p}}^{k+1}\|_{\mathbf{P}_{\theta_*}}^2 \leq \text{rate}^2(\lambda, R) \leq \frac{1}{\frac{(c_K^2 + \lambda) \left(1 + \frac{2\beta_d^2(\beta_s^{-2} + \lambda)R}{n}\right)}{(\beta_s^{-2} + \lambda)} + 1} \leq \max \left\{ \frac{\beta_s^{-2}}{c_K^2 + \beta_s^{-2}}, \frac{1}{2} \right\},$$

where

$$(3.16) \quad \|\mathbf{e}_{\mathbf{p}}^{k+1}\|_{\mathbf{P}_{\theta_*}}^2 := \|\Lambda_4^{\frac{1}{2}} \mathbf{e}_{\mathbf{p}}^{k+1}\|^2 + \frac{2(\beta_s^{-2} + \lambda)\beta_v^2}{\lambda_0} \|\Lambda_3^{\frac{1}{2}} \mathbf{e}_{\mathbf{p}}^{k+1}\|^2 + \|(\Lambda_1 + \Lambda_2)^{\frac{1}{2}} \mathbf{e}_{\mathbf{p}}^{k+1}\|^2.$$

Proof. In view of the estimate presented in Lemma 3.2, we want to find L_2 and L_1 subject to the condition

$$(3.17) \quad \frac{\lambda_0}{2(c_K^2 + \lambda)} - \frac{L_2}{2} - \frac{L_1 R \lambda_0}{2n} \leq 0.$$

For any $\theta > 0$, we rewrite (3.12) as

$$(3.18) \quad \begin{aligned} & \frac{\lambda_0}{2(\beta_s^{-2} + \lambda)} \|\Lambda_4^{\frac{1}{2}} \mathbf{e}_{\mathbf{p}}^{k+1}\|^2 + \theta^{-1} \theta \beta_d^2 \|\Lambda_3^{\frac{1}{2}} \mathbf{e}_{\mathbf{p}}^{k+1}\|^2 + \|(\Lambda_1 + \Lambda_2)^{\frac{1}{2}} \mathbf{e}_{\mathbf{p}}^{k+1}\|^2 + \frac{L_1}{2\theta \beta_d^2} \theta \beta_d^2 \|\Lambda_3^{\frac{1}{2}} \mathbf{e}_{\mathbf{p}}^{k+1}\|^2 + \frac{L_2}{2} \|\Lambda_4^{\frac{1}{2}} \mathbf{e}_{\mathbf{p}}^{k+1}\|^2 \\ & \leq \frac{L_1}{2\theta \beta_d^2} \theta \beta_d^2 \|\Lambda_3^{\frac{1}{2}} \mathbf{e}_{\mathbf{p}}^k\|^2 + \frac{L_2}{2} \|\Lambda_4^{\frac{1}{2}} \mathbf{e}_{\mathbf{p}}^k\|^2 + \left(\frac{\lambda_0}{2(c_K^2 + \lambda)} - \frac{L_2}{2} - \frac{L_1 R \lambda_0}{2n} \right) \|\Lambda_4^{\frac{1}{2}} (\mathbf{e}_{\mathbf{p}}^{k+1} - \mathbf{e}_{\mathbf{p}}^k)\|^2, \end{aligned}$$

namely,

$$(3.19) \quad \begin{aligned} & \left(\frac{\lambda_0}{2(\beta_s^{-2} + \lambda)} + \frac{L_2}{2} \right) \|\Lambda_4^{\frac{1}{2}} \mathbf{e}_{\mathbf{p}}^{k+1}\|^2 + \left(\theta^{-1} + \frac{L_1}{2\theta \beta_d^2} \right) \theta \beta_d^2 \|\Lambda_3^{\frac{1}{2}} \mathbf{e}_{\mathbf{p}}^{k+1}\|^2 + \|(\Lambda_1 + \Lambda_2)^{\frac{1}{2}} \mathbf{e}_{\mathbf{p}}^{k+1}\|^2 \\ & \leq \frac{L_1}{2\theta \beta_d^2} \theta \beta_d^2 \|\Lambda_3^{\frac{1}{2}} \mathbf{e}_{\mathbf{p}}^k\|^2 + \frac{L_2}{2} \|\Lambda_4^{\frac{1}{2}} \mathbf{e}_{\mathbf{p}}^k\|^2. \end{aligned}$$

Then, for $L_2 \leq 1$ we obtain

$$(3.20) \quad \begin{aligned} & \min \left\{ \frac{\lambda_0}{2(\beta_s^{-2} + \lambda)} + \frac{L_2}{2}, \theta^{-1} + \frac{L_1}{2\theta\beta_d^2} \right\} \left(\|\Lambda_4^{\frac{1}{2}} \mathbf{e}_{\mathbf{p}}^{k+1}\|^2 + \theta\beta_d^2 \|\Lambda_3^{\frac{1}{2}} \mathbf{e}_{\mathbf{p}}^{k+1}\|^2 + \|(\Lambda_1 + \Lambda_2)^{\frac{1}{2}} \mathbf{e}_{\mathbf{p}}^{k+1}\|^2 \right) \\ & \leq \max \left\{ \frac{L_1}{2\theta\beta_d^2}, \frac{L_2}{2} \right\} \left(\theta\beta_d^2 \|\Lambda_3^{\frac{1}{2}} \mathbf{e}_{\mathbf{p}}^k\|^2 + \|\Lambda_4^{\frac{1}{2}} \mathbf{e}_{\mathbf{p}}^k\|^2 \right). \end{aligned}$$

Now, choose $L_1 = \theta\beta_d^2 L_2$. Then, condition (3.17) becomes

$$(3.21) \quad \frac{\lambda_0}{2(c_K^2 + \lambda)} - \frac{L_2}{2} - \frac{\theta\beta_d^2 L_2 R \lambda_0}{2n} \leq 0 \text{ or } L_2 \geq \frac{\frac{\lambda_0}{(c_K^2 + \lambda)}}{1 + \frac{\theta\beta_d^2 R \lambda_0}{n}}$$

and we can simplify (3.20) as follows

$$\begin{aligned} & \min \left\{ \frac{\lambda_0}{2(\beta_s^{-2} + \lambda)} + \frac{L_2}{2}, \theta^{-1} + \frac{L_2}{2} \right\} \left(\|\Lambda_4^{\frac{1}{2}} \mathbf{e}_{\mathbf{p}}^{k+1}\|^2 + \theta\beta_d^2 \|\Lambda_3^{\frac{1}{2}} \mathbf{e}_{\mathbf{p}}^{k+1}\|^2 + \|(\Lambda_1 + \Lambda_2)^{\frac{1}{2}} \mathbf{e}_{\mathbf{p}}^{k+1}\|^2 \right) \\ & \leq \frac{L_2}{2} \left(\theta\beta_d^2 \|\Lambda_3^{\frac{1}{2}} \mathbf{e}_{\mathbf{p}}^k\|^2 + \|\Lambda_4^{\frac{1}{2}} \mathbf{e}_{\mathbf{p}}^k\|^2 \right), \end{aligned}$$

which shows (3.13). Statements 1. and 2. are direct consequences of (3.13) for the particular choices of θ in the corresponding norms. \square

Note that estimate (3.15) not only indicates that the convergence rate of the Uzawa-type iterative method has a uniform, with respect to the parameters, upper-bound being strictly less than 1, but also that it is bounded by a number much smaller than 1 if λ is large. Moreover, the presented analysis of the Uzawa-type scheme results in a new, parameter-optimized block-triangular preconditioner that can be used to accelerate the convergence of the GMRES method if the latter is applied to the augmented system (2.13). The parameter-robust uniform convergence estimates for the new Uzawa-type method imply the field-of-values equivalence of this preconditioner for the augmented system.

Theorem 3.4. *Consider Algorithm 1 with S as introduced in (2.28). Then the errors $\mathbf{e}_{\mathbf{u}}^k$ and $\mathbf{e}_{\mathbf{v}}^k$ defined in (2.23) satisfy the estimates:*

$$(3.22) \quad \|\mathbf{e}_{\mathbf{u}}^k\|_{\mathbf{U}} \leq C_u [\text{rate}(\lambda, R)]^k, \quad \|\mathbf{e}_{\mathbf{v}}^k\|_{\mathbf{V}_{\theta^*}} \leq C_v [\text{rate}(\lambda, R)]^k$$

where

$$(3.23) \quad \|\mathbf{e}_{\mathbf{v}}^k\|_{\mathbf{V}_{\theta^*}}^2 := (A_{\mathbf{v}} \mathbf{e}_{\mathbf{v}}^k, \mathbf{e}_{\mathbf{v}}^k) + (S^{-1} \text{Div} \mathbf{e}_{\mathbf{v}}^k, \text{Div} \mathbf{e}_{\mathbf{v}}^k), \quad \|\mathbf{u}\|_{\mathbf{U}}^2 := \|\boldsymbol{\epsilon}(\mathbf{u})\|^2 + \lambda \|\text{div} \mathbf{u}\|^2$$

and the constants C_u and C_v are independent of the model parameters and the time step size.

Proof. First, we estimate $\|\mathbf{e}_{\mathbf{u}}^{k+1}\|_{\mathbf{U}}^2$. By setting $\mathbf{w} = \mathbf{e}_{\mathbf{u}}^{k+1}$ in (2.24c), applying Cauchy's inequality and using (3.8) we obtain

$$\begin{aligned} \|\boldsymbol{\epsilon}(\mathbf{e}_{\mathbf{u}}^{k+1})\|^2 + \lambda \|\text{div} \mathbf{e}_{\mathbf{u}}^{k+1}\|^2 &= \left(\sum_{i=1}^n \mathbf{e}_{p_i}^{k+1}, \text{div} \mathbf{e}_{\mathbf{u}}^{k+1} \right) \leq \left\| \sum_{i=1}^n \mathbf{e}_{p_i}^{k+1} \right\| \cdot \|\text{div} \mathbf{e}_{\mathbf{u}}^{k+1}\| = \sqrt{\lambda_0} \|\Lambda_4^{\frac{1}{2}} \mathbf{e}_{\mathbf{p}}^{k+1}\| \cdot \|\text{div} \mathbf{e}_{\mathbf{u}}^{k+1}\| \\ &\leq \sqrt{\lambda_0} \|\Lambda_4^{\frac{1}{2}} \mathbf{e}_{\mathbf{p}}^{k+1}\| \cdot \sqrt{\frac{1}{c_K^2 + \lambda} (\|\boldsymbol{\epsilon}(\mathbf{e}_{\mathbf{u}}^{k+1})\|^2 + \lambda \|\text{div} \mathbf{e}_{\mathbf{u}}^{k+1}\|^2)}, \end{aligned}$$

or, equivalently,

$$(3.24) \quad \|\mathbf{e}_{\mathbf{u}}^{k+1}\|_{\mathbf{U}}^2 \leq \frac{\lambda_0}{c_K^2 + \lambda} \|\Lambda_4^{\frac{1}{2}} \mathbf{e}_{\mathbf{p}}^{k+1}\|^2 \leq \frac{\lambda_0}{c_K^2 + \lambda} \|\mathbf{e}_{\mathbf{p}}^{k+1}\|_{\mathbf{P}_{\theta}}^2.$$

In order to estimate $\|\mathbf{e}_v^{k+1}\|_{\mathbf{V}_{\theta_*}}^2$ we set $\mathbf{z} = \mathbf{e}_v^{k+1}$ in (2.24a) and apply the Cauchy inequality to derive

$$\begin{aligned}
(A_v \mathbf{e}_v^{k+1}, \mathbf{e}_v^{k+1}) + (S^{-1} \text{Div} \mathbf{e}_v^{k+1}, \text{Div} \mathbf{e}_v^{k+1}) &= (\mathbf{e}_p^k, \text{Div} \mathbf{e}_v^{k+1}) - (S^{-1} \underline{\text{Div}} \mathbf{e}_u^k, \text{Div} \mathbf{e}_v^{k+1}) - (S^{-1}(\Lambda_1 + \Lambda_2) \mathbf{e}_p^k, \text{Div} \mathbf{e}_v^{k+1}) \\
&= (S^{-1}(L_1 \Lambda_3 + L_2 \Lambda_4) \mathbf{e}_p^k, \text{Div} \mathbf{e}_v^{k+1}) - (S^{-1} \underline{\text{Div}} \mathbf{e}_u^k, \text{Div} \mathbf{e}_v^{k+1}) \\
&\leq (S^{-1}(L_1 \Lambda_3 + L_2 \Lambda_4) \mathbf{e}_p^k, (L_1 \Lambda_3 + L_2 \Lambda_4) \mathbf{e}_p^k) \\
&\quad + \frac{1}{4} (S^{-1} \text{Div} \mathbf{e}_v^{k+1}, \text{Div} \mathbf{e}_v^{k+1}) + (S^{-1} \underline{\text{Div}} \mathbf{e}_u^k, \underline{\text{Div}} \mathbf{e}_u^k) + \frac{1}{4} (S^{-1} \text{Div} \mathbf{e}_v^{k+1}, \text{Div} \mathbf{e}_v^{k+1}).
\end{aligned}
\tag{3.25}$$

From the definition of S , see (2.28), that of $\|\cdot\|_{\mathbf{P}_{\theta_*}}$, see (3.16), and noting that $L_1 = \theta \beta_d^2 L_2$, see Theorem 6, we have

$$\begin{aligned}
(S^{-1}(L_1 \Lambda_3 + L_2 \Lambda_4) \mathbf{e}_p^k, (L_1 \Lambda_3 + L_2 \Lambda_4) \mathbf{e}_p^k) &\leq ((L_1 \Lambda_3 + L_2 \Lambda_4)^{-1} (L_1 \Lambda_3 + L_2 \Lambda_4) \mathbf{e}_p^k, (L_1 \Lambda_3 + L_2 \Lambda_4) \mathbf{e}_p^k) \\
&= ((L_1 \Lambda_3 + L_2 \Lambda_4) \mathbf{e}_p^k, \mathbf{e}_p^k) \leq L_2 \|\mathbf{e}_p^k\|_{\mathbf{P}_{\theta_*}}^2.
\end{aligned}
\tag{3.26}$$

Then (3.25) can be rewritten in the form

$$(A_v \mathbf{e}_v^{k+1}, \mathbf{e}_v^{k+1}) + \frac{1}{2} (S^{-1} \text{Div} \mathbf{e}_v^{k+1}, \text{Div} \mathbf{e}_v^{k+1}) \leq L_2 \|\mathbf{e}_p^k\|_{\mathbf{P}_{\theta_*}}^2 + \|S^{-\frac{1}{2}} \underline{\text{Div}} \mathbf{e}_u^k\|^2.
\tag{3.27}$$

Again, from the definition of S , and observing that $L_1 \Lambda_3 + L_2 \Lambda_4 = (L_1 R I_{n \times n} + \frac{L_2}{\lambda_0} \mathbf{e} \mathbf{e}^T)$, then by choosing $a = L_1 R$ and $b = \frac{L_2}{\lambda_0}$ in Lemma 2.1, it follows that

$$\|S^{-\frac{1}{2}} \underline{\text{Div}} \mathbf{e}_u^k\|^2 \leq ((L_1 \Lambda_3 + L_2 \Lambda_4)^{-1} \underline{\text{Div}} \mathbf{e}_u^k, \underline{\text{Div}} \mathbf{e}_u^k) = \left(\sum_{i=1}^n \sum_{j=1}^n b_{ij} \right) \text{div} \mathbf{e}_u^k, \text{div} \mathbf{e}_u^k
\tag{3.28}$$

$$= \frac{n \lambda_0}{L_1 R \lambda_0 + n L_2} (\text{div} \mathbf{e}_u^k, \text{div} \mathbf{e}_u^k) \leq (c_K^2 + \lambda) (\text{div} \mathbf{e}_u^k, \text{div} \mathbf{e}_u^k).
\tag{3.29}$$

Therefore, from (3.24), we have

$$\begin{aligned}
\|\mathbf{e}_v^k\|_{\mathbf{V}_{\theta_*}}^2 &= (A_v \mathbf{e}_v^{k+1}, \mathbf{e}_v^{k+1}) + \frac{1}{2} (S^{-1} \text{Div} \mathbf{e}_v^{k+1}, \text{Div} \mathbf{e}_v^{k+1}) \leq L_2 \|\mathbf{e}_p^k\|_{\mathbf{P}_{\theta_*}}^2 + (c_K^2 + \lambda) (\text{div} \mathbf{e}_u^k, \text{div} \mathbf{e}_u^k) \leq L_2 \|\mathbf{e}_p^k\|_{\mathbf{P}_{\theta_*}}^2 + \|\mathbf{e}_u^k\|_U^2 \\
&\leq L_2 \|\mathbf{e}_p^k\|_{\mathbf{P}_{\theta_*}}^2 + \frac{\lambda_0}{c_K^2 + \lambda} \|\mathbf{e}_p^k\|_{\mathbf{P}_{\theta_*}}^2 = \left(L_2 + \frac{\lambda_0}{c_K^2 + \lambda} \right) \|\mathbf{e}_p^k\|_{\mathbf{P}_{\theta_*}}^2,
\end{aligned}$$

which completes the proof. \square

Remark 3.5. Note that for the particular choice of S and M in this section, the block triangular matrix on the left-hand side of (2.16) provides a field of values equivalent preconditioner with equivalence constants independent of any model and discretization parameters.

4. THE DISCRETE MPET PROBLEM

Mass conservative discretizations for the MPET model are considered in this section, cf. [27, 28]. The analysis here can also be utilized for other stable discretizations of the three-field formulation of the MPET model, e.g. [31, 46].

4.1. Notation. Let \mathcal{T}_h be a shape-regular triangulation of the domain Ω into triangles/tetrahedrons where the subscript h denotes the mesh-size. Furthermore, let \mathcal{E}_h^I and \mathcal{E}_h^B define the set of all interior edges/faces and the set of all boundary edges/faces of \mathcal{T}_h respectively with their union being written as \mathcal{E}_h .

We introduce the following broken Sobolev spaces

$$H^s(\mathcal{T}_h) = \{\phi \in L^2(\Omega), \text{ such that } \phi|_T \in H^s(T) \text{ for all } T \in \mathcal{T}_h\}$$

for $s \geq 1$.

Define T_1 and T_2 to be two elements from the triangulation which share an edge or face e and \mathbf{n}_1 and \mathbf{n}_2 to be the corresponding unit normal vectors to e which point to the exterior of T_1 and T_2 . For $q \in H^1(\mathcal{T}_h)$, $\mathbf{v} \in H^1(\mathcal{T}_h)^d$ and $\boldsymbol{\tau} \in H^1(\mathcal{T}_h)^{d \times d}$ and any $e \in \mathcal{E}_h^I$, the jumps $[\cdot]$ and averages $\{\cdot\}$ are defined by

$$[q] = q|_{\partial T_1 \cap e} - q|_{\partial T_2 \cap e}, \quad [\mathbf{v}] = \mathbf{v}|_{\partial T_1 \cap e} - \mathbf{v}|_{\partial T_2 \cap e}$$

and

$$\{\mathbf{v}\} = \frac{1}{2}(\mathbf{v}|_{\partial T_1 \cap e} \cdot \mathbf{n}_1 - \mathbf{v}|_{\partial T_2 \cap e} \cdot \mathbf{n}_2), \quad \{\boldsymbol{\tau}\} = \frac{1}{2}(\boldsymbol{\tau}|_{\partial T_1 \cap e} \mathbf{n}_1 - \boldsymbol{\tau}|_{\partial T_2 \cap e} \mathbf{n}_2),$$

whereas in the case of $e \in \mathcal{E}_h^B$

$$[q] = q|_e, \quad [\mathbf{v}] = \mathbf{v}|_e, \quad \{\mathbf{v}\} = \mathbf{v}|_e \cdot \mathbf{n}, \quad \{\boldsymbol{\tau}\} = \boldsymbol{\tau}|_e \mathbf{n}.$$

4.2. Mixed finite element spaces and discrete formulation. So as to discretize the flow equations, a mixed finite element method has been used to approximate fluxes and pressures. The displacement field of the mechanics problem is approximated using a discontinuous Galerkin method. The following finite element spaces are employed:

$$\begin{aligned} \mathbf{U}_h &= \{\mathbf{u} \in H(\text{div}; \Omega) : \mathbf{u}|_T \in \mathbf{U}(T), T \in \mathcal{T}_h; \mathbf{u} \cdot \mathbf{n} = 0 \text{ on } \partial\Omega\}, \\ \mathbf{V}_{i,h} &= \{\mathbf{v} \in H(\text{div}; \Omega) : \mathbf{v}|_T \in \mathbf{V}_i(T), T \in \mathcal{T}_h; \mathbf{v} \cdot \mathbf{n} = 0 \text{ on } \partial\Omega\}, i = 1, \dots, n, \\ P_{i,h} &= \left\{ q \in L^2(\Omega) : q|_T \in Q_i(T), T \in \mathcal{T}_h; \int_{\Omega} q dx = 0 \right\}, i = 1, \dots, n, \end{aligned}$$

where $\mathbf{V}_i(T)/Q_i(T) = \text{RT}_{l-1}(T)/\text{P}_{l-1}(T)$, $\mathbf{U}(T) = \text{BDM}_l(T)$ or $\mathbf{U}(T) = \text{BDFM}_l(T)$ for $l \geq 1$. One should note that $\text{div } \mathbf{U}(T) = \text{div } \mathbf{V}_i(T) = Q_i(T)$ for each of these choices.

Also, it has been shown in [27, 28] that for all $\mathbf{u} \in \mathbf{U}_h$, $[\mathbf{u}_n] = 0$, from which follows that $[\mathbf{u}] = [\mathbf{u}_t]$. Here, \mathbf{u}_n and \mathbf{u}_t are the normal and tangential component of \mathbf{u} respectively.

Defining

$$\begin{aligned} \mathbf{v}_h^T &= (\mathbf{v}_{1,h}^T, \dots, \mathbf{v}_{n,h}^T), & \mathbf{p}_h^T &= (p_{1,h}, \dots, p_{n,h}), \\ \mathbf{z}_h^T &= (\mathbf{z}_{1,h}^T, \dots, \mathbf{z}_{n,h}^T), & \mathbf{q}_h^T &= (q_{1,h}, \dots, q_{n,h}), \\ \mathbf{V}_h &= \mathbf{V}_{1,h} \times \dots \times \mathbf{V}_{n,h}, & \mathbf{P}_h &= P_{1,h} \times \dots \times P_{n,h}, & \mathbf{X}_h &= \mathbf{U}_h \times \mathbf{V}_h \times \mathbf{P}_h, \end{aligned}$$

then the following discretization of the continuous variational problem results from the weak formulation of (2.6): Find $(\mathbf{u}_h; \mathbf{v}_h; \mathbf{p}_h) \in \mathbf{X}_h$, such that for any $(\mathbf{w}_h; \mathbf{z}_h; \mathbf{q}_h) \in \mathbf{X}_h$ and $i = 1, \dots, n$

$$(4.1a) \quad (R_i^{-1} \mathbf{v}_{i,h}, \mathbf{z}_{i,h}) - (p_{i,h}, \text{div } \mathbf{z}_{i,h}) = 0,$$

$$(4.1b) \quad -(\text{div } \mathbf{u}_h, q_{i,h}) - (\text{div } \mathbf{v}_{i,h}, q_{i,h}) + \tilde{\alpha}_{ii}(p_{i,h}, q_{i,h}) + \sum_{\substack{j=1 \\ j \neq i}}^n \alpha_{ij}(p_{j,h}, q_{i,h}) = (g_i, q_{i,h}),$$

$$(4.1c) \quad a_h(\mathbf{u}_h, \mathbf{w}_h) + \lambda(\text{div } \mathbf{u}_h, \text{div } \mathbf{w}_h) - \sum_{i=1}^n (p_{i,h}, \text{div } \mathbf{w}_h) = (\mathbf{f}, \mathbf{w}_h),$$

where

$$(4.2) \quad \begin{aligned} a_h(\mathbf{u}, \mathbf{w}) &= \sum_{T \in \mathcal{T}_h} \int_T \mathbf{e}_p(\mathbf{u}) : \mathbf{e}_p(\mathbf{w}) dx - \sum_{e \in \mathcal{E}_h} \int_e \{\mathbf{e}_p(\mathbf{u})\} \cdot [\mathbf{w}_t] ds \\ &\quad - \sum_{e \in \mathcal{E}_h} \int_e \{\mathbf{e}_p(\mathbf{w})\} \cdot [\mathbf{u}_t] ds + \sum_{e \in \mathcal{E}_h} \int_e \eta h_e^{-1} [\mathbf{u}_t] \cdot [\mathbf{w}_t] ds, \end{aligned}$$

$\tilde{\alpha}_{ii} = -\alpha_{p_i} - \alpha_{ii}$, and η is a stabilization parameter which is independent of λ , R_i^{-1} , α_{p_i} , α_{ij} , $i, j \in \{1, \dots, n\}$, the network scale n , and the mesh size h .

In the derivation of the discrete variational problem (4.1), homogeneous Dirichlet boundary conditions for \mathbf{u} and homogeneous Neumann boundary conditions for p_i , $i = 1, 2, \dots, n$, have been assumed for each case over the entire domain boundary. The DG discretizations for more general (rescaled) boundary conditions and the stability analysis of the related discrete variational problems can be found in [28, 27]. The iterative scheme for flux-pressure-displacement formulation of the discrete MPET problem, analogous to Algorithm 1, is as follows:

Algorithm 2 Fully decoupled iterative scheme for flux-pressure-displacement formulation of discrete MPET problem

Step a: Given \mathbf{p}_h^k and \mathbf{u}_h^k , we first solve for \mathbf{v}_h^{k+1} , such that for all $\mathbf{z}_h \in \mathbf{V}_h$ there holds

$$(4.3) \quad (A_v \mathbf{v}_h^{k+1}, \mathbf{z}_h) + (M \text{Div} \mathbf{v}_h^{k+1}, \text{Div} \mathbf{z}_h) = -(M \mathbf{g}, \text{Div} \mathbf{z}_h) + ((I - M(\Lambda_1 + \Lambda_2)) \mathbf{p}_h^k, \text{Div} \mathbf{z}_h) - (M \underline{\text{Div}} \mathbf{u}_h^k, \text{Div} \mathbf{z}_h).$$

Step b: Given \mathbf{u}_h^k and \mathbf{v}_h^{k+1} , we solve for \mathbf{p}_h^{k+1} , such that for all $\mathbf{q}_h \in \mathbf{P}_h$ there holds

$$(4.4) \quad (S \mathbf{p}_h^{k+1}, \mathbf{q}_h) = -(\mathbf{g}, \mathbf{q}_h) + (S \mathbf{p}_h^k, \mathbf{q}_h) - ((\Lambda_1 + \Lambda_2) \mathbf{p}_h^k, \mathbf{q}_h) - (\underline{\text{Div}} \mathbf{u}_h^k, \mathbf{q}_h) - (\text{Div} \mathbf{v}_h^{k+1}, \mathbf{q}_h).$$

Step c: Given \mathbf{p}_h^{k+1} and \mathbf{v}_h^{k+1} , we solve for \mathbf{u}_h^{k+1} , such that for all $\mathbf{w}_h \in \mathbf{U}_h$ there holds

$$(4.5) \quad a_h(\mathbf{u}_h^{k+1}, \mathbf{w}_h) = (\mathbf{f}, \mathbf{w}_h) + (\mathbf{p}_h^{k+1}, \underline{\text{Div}} \mathbf{w}_h).$$

In **Step a**, a coupled $H(\text{div})$ problem is solved. As mentioned in Remark 6 of [28], we can apply orthogonal transformations to the flux and pressure subsystems which decouple the fluxes from each other and also the pressures from each other. For fluxes, this procedure results in n decoupled $H(\text{div})$ problems for the operators $I + \bar{\mu}_i \nabla \text{div}$, $i = 1, 2, \dots, n$, where $\bar{\mu}_i$ are the eigenvalues of an $n \times n$ coefficient matrix, n denoting the number of networks, i.e., $n \in \{1, 2, 4, 8\}$ in the examples presented in the next section; correspondingly, the decoupling of the pressure subsystem yields n , essentially, well conditioned independent L^2 problems.

There are several works addressing the solution of nearly singular $H(\text{div})$ problems and we may resort to Hiptmair-Xu preconditioners [26] and the robust subspace correction methods [57, 58, 39, 41]. There also exist multigrid methods that serve this purpose, see, e.g. [55, 5]. In case of highly varying permeability (conductivity) coefficient, the auxiliary space multigrid preconditioners based on additive Schur complement approximation proposed by Kraus et al. [35] provide a parameter-robust alternative.

In **Step c**, to obtain A_u^{-1} for the elasticity subproblem, one can use the multigrid method proposed in [30] for the discontinuous Galerkin discretization and the multigrid methods proposed in [47, 40] for conforming elements, which are all robust with respect to the Lamé parameter λ . Following the methodology of the convergence analysis presented for the continuous MPET problem, statements analogous to those presented in Theorem 3.3 and Theorem 3.4 can also be proven for Algorithm 2.

5. NUMERICAL RESULTS

In the following, we consider four numerical test settings to demonstrate the effectiveness and accuracy of the proposed Uzawa-type iterative schemes for the MPET model.

First, numerical results are presented for the single network problem, i.e., the Biot model, in Figure 1. These validate the theoretical convergence estimates of the linear stationary iterative method based on Algorithm 1 which has been additionally assessed against the preconditioned GMRES algorithm. In the second and third tests, the performance of Algorithm 1 is compared with the preconditioned GMRES algorithm and the fixed-stress algorithm as proposed in [29], cf. (2.10), for the two-network and four-network MPET problems. Finally, a scaling test demonstrating the behaviour of the preconditioned GMRES and the Uzawa-type algorithms for different numbers of networks is performed.

The block Gauss-Seidel preconditioner that we have used to accelerate the GMRES method equals the lower block triangular matrix in the left-hand side of (2.16) where $M = S^{-1}$ and S is given in (2.28).

All the numerical results in this section have been conducted on the FEniCS computing platform, see e.g. [4, 42]. In all test cases the set-up is as follows:

- The domain $\Omega \in \mathbb{R}^2$ is the unit square which is partitioned into $2N^2$ congruent right-angled triangles;
- The discretization setting is the same as in [29, 28], i.e., we use discontinuous piecewise constant elements, lowest-order Raviart-Thomas elements and Brezzi-Douglas-Marini elements to approximate the pressures, fluxes and displacement fields respectively;
- For all experiments conducted using Algorithm 1 we set

$$L_2 = \frac{\lambda_0}{(c_k^2 + \lambda)(1 + \frac{2\beta_d^2(\beta_s^{-2} + \lambda)R}{n})}, \quad L_1 = \frac{2(\beta_s^{-2} + \lambda)\beta_d^2}{\lambda_0} L_2$$

and $\beta_s^2 = \beta_d^2 = 0.18$, see [21].

- The stopping criterium of the iterative process is the reduction of the initial preconditioned residual by a factor 10^8 where a random vector has been used in the initialization.

5.1. The Biot's consolidation model. Consider system (2.1) for $n = 1$, i.e., a system for which only one pressure and one flux exists, where for $(x, y) \in \Omega$

$$g = R_1 \left(\frac{\partial \phi_2}{\partial x} + \frac{\partial \phi_2}{\partial y} \right) - \alpha_{p_1}(\phi_2 - 1),$$

$$\phi_1 = (x - 1)^2(y - 1)^2x^2y^2, \quad \phi_2 = 900(x - 1)^2(y - 1)^2x^2y^2$$

and

$$\mathbf{f} = \begin{pmatrix} -(2y^3 - 3y^2 + y)(12x^2 - 12x + 2) - (x - 1)^2x^2(12y - 6) + 900(y - 1)^2y^2(4x^3 - 6x^2 + 2x) \\ (2x^3 - 3x^2 + x)(12y^2 - 12y + 2) + (y - 1)^2y^2(12x - 6) + 900(x - 1)^2x^2(4y^3 - 6y^2 + 2y) \end{pmatrix}.$$

Experiments over a wide-range of input parameters α_p , λ , R_1^{-1} have been run with Algorithm 1 and the preconditioned GMRES algorithm and are shown in Figure 1. In all test cases, the number of Uzawa-type iterations required to achieve the prescribed solution accuracy is bounded by a constant independent of all model and discretization parameters. Clearly, the GMRES preconditioned algorithm demonstrates better convergence behaviour for small λ .

5.2. The Biot-Barenblatt model. In the next test, system (2.1) is considered for $n = 2$ where the problem setting is as per the cantilever bracket benchmark problem in [23]. We denote the bottom, right, top and left parts of $\Gamma = \partial\Omega$ by Γ_1 , Γ_2 , Γ_3 and Γ_4 and, also, we impose $\mathbf{u} = 0$ on Γ_4 , $(\boldsymbol{\sigma} - p_1\mathbf{I} - p_2\mathbf{I})\mathbf{n} = (0, 0)^T$ on $\Gamma_1 \cup \Gamma_2$, $(\boldsymbol{\sigma} - p_1\mathbf{I} - p_2\mathbf{I})\mathbf{n} = (0, -1)^T$ on Γ_3 , $p_1 = 2$ on Γ and $p_2 = 20$ on Γ . Further, we set $\mathbf{f} = \mathbf{0}$, $g_1 = 0$ and $g_2 = 0$. Table 1 shows the reference values of the model parameters as given in [34].

Figures 2–4 present a comparison between the preconditioned GMRES algorithm, the fixed-stress split algorithm as presented in [29] with a tuning parameter $L = 1/(1 + \lambda)$ and Algorithm 1. As can be seen, from Figures 2 and 4 for λ being sufficiently large, the Uzawa-type method shows similar convergence behaviour to the preconditioned GMRES and fixed-stress methods.

Furthermore, all the numerical results included in Figures 2–4 demonstrate the robust performance of the Uzawa-type algorithm with respect to mesh refinements and variation of the hydraulic conductivities K_1 and K_2 , and λ .

5.3. The four-network model. Now we consider system (2.1) for $n = 4$. This test setting is analogous to the previous example, i.e., $\partial\Omega = \bar{\Gamma}_1 \cup \bar{\Gamma}_2 \cup \bar{\Gamma}_3 \cup \bar{\Gamma}_4$ with Γ_1 , Γ_2 , Γ_3 , Γ_4 denoting the bottom, right, top and left boundaries respectively, $\mathbf{u} = 0$ on Γ_4 , $(\boldsymbol{\sigma} - p_1\mathbf{I} - p_2\mathbf{I} - p_3\mathbf{I} - p_4\mathbf{I})\mathbf{n} = (0, 0)^T$ on $\Gamma_1 \cup \Gamma_2$, $(\boldsymbol{\sigma} - p_1\mathbf{I} - p_2\mathbf{I} - p_3\mathbf{I} - p_4\mathbf{I})\mathbf{n} = (0, -1)^T$ on Γ_3 , $p_1 = 2$ on Γ , $p_2 = 20$ on Γ , $p_3 = 30$ on Γ , $p_4 = 40$ on Γ . All right-hand sides have been chosen to be zero. The reference values of the parameters are taken from [53] and presented in Table 2.

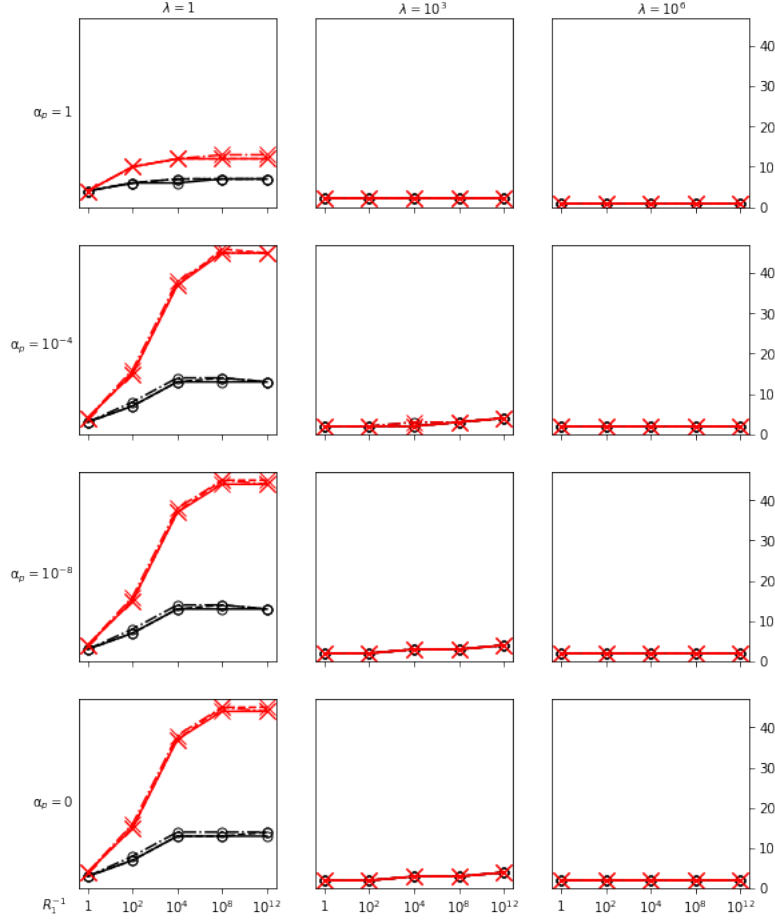


FIGURE 1. Number of preconditioned GMRES (small black circles) and augmented Uzawa-type (red crosses) iterations for preconditioned residual reduction by a factor 10^8 when solving the Biot problem. These tests have been performed for $h = 1/32$ (dash-dotted line), $h = 1/64$ (dashed line) and $h = 1/128$ (full line).

The main aim of the numerical experiments discussed in this subsection is, again, the comparison between the three algorithms, namely the preconditioned GMRES algorithm, the fixed-stress split algorithm with $L = 1/(1 + \lambda)$ and the fully decoupling Algorithm 1.

Figure 5 shows that Algorithm 1 exhibits a convergence behaviour similar to that of the preconditioned GMRES method and the fixed-stress split iterative scheme over a wide-range of parameters as tabulated. Moreover, the presented numerical results demonstrate the robustness of the newly proposed algorithm with respect to large variations of the coefficients K_3 , $K = K_1 = K_2 = K_4$ and λ and the mesh parameter h .

In order to further compare the performance of the preconditioned GMRES, fixed-stress split and augmented Uzawa-type algorithms we present one final table, Table 3, with elapsed times measured in seconds. These numerical tests have been conducted on a Dell Precision 5540 notebook with an Intel Core i7-9 9850H processor and 64GB RAM. As

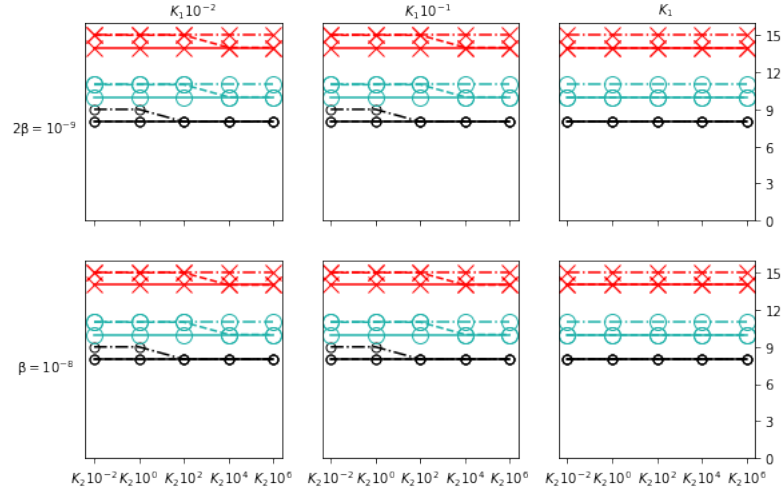


FIGURE 2. Number of preconditioned GMRES (small black circles), fixed-stress split (big green circles) and augmented Uzawa-type (red crosses) iterations for preconditioned residual reduction by a factor 10^8 when solving the Barenblatt problem, $\lambda = \hat{\lambda}$. These tests have been performed for $h = 1/16$ (dash-dotted line), $h = 1/32$ (dashed line) and $h = 1/64$ (full line).

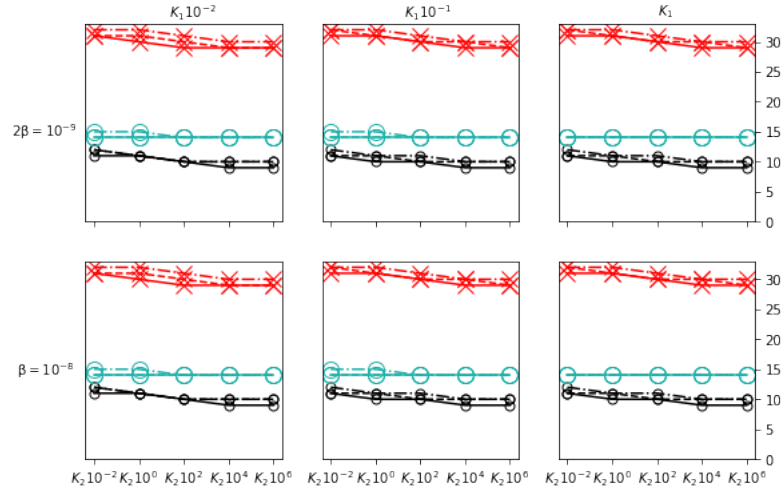


FIGURE 3. Number of preconditioned GMRES (small black circles), fixed-stress split (big green circles) and augmented Uzawa-type (red crosses) iterations for preconditioned residual reduction by a factor 10^8 when solving the Barenblatt problem, $\lambda := 0.01 * \hat{\lambda}$. These tests have been performed for $h = 1/16$ (dash-dotted line), $h = 1/32$ (dashed line) and $h = 1/64$ (full line).

TABLE 1. Reference values of model parameters for the Barenblatt model.

parameter	value	unit
$\hat{\lambda}$	$4.2 * 10^6$	Nm^{-2}
μ	$2.4 * 10^6$	Nm^{-2}
c_{p1}	$5.4 * 10^{-8}$	N^{-1}m^2
c_{p2}	$1.4 * 10^{-8}$	N^{-1}m^2
α_1	0.95	
α_2	0.12	
β	$5.0 * 10^{-10}$	$\text{N}^{-1}\text{m}^2\text{s}^{-1}$
	$1.0 * 10^{-8}$	$\text{N}^{-1}\text{m}^2\text{s}^{-1}$
K_1	$6.18 * 10^{-12}$	$\text{N}^{-1}\text{m}^4\text{s}^{-1}$
K_2	$2.72 * 10^{-11}$	$\text{N}^{-1}\text{m}^4\text{s}^{-1}$

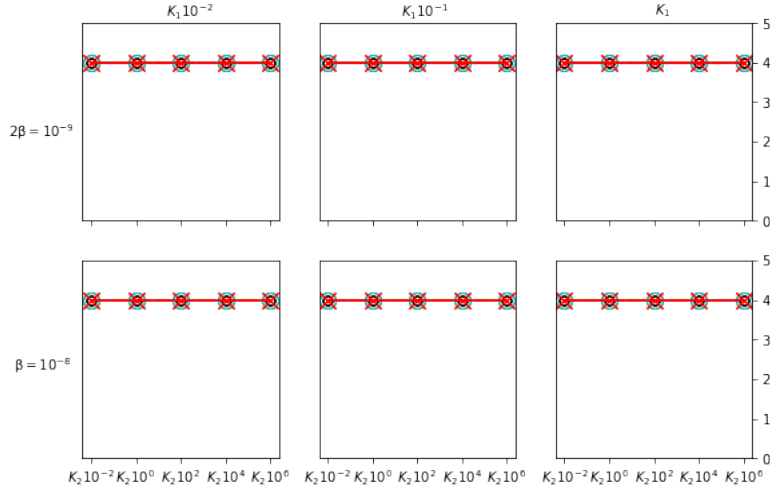


FIGURE 4. Number of preconditioned GMRES (small black circles), fixed-stress split (big green circles) and augmented Uzawa-type (red crosses) iterations for preconditioned residual reduction by a factor 10^8 when solving the Barenblatt problem, $\lambda := 100 * \hat{\lambda}$. These tests have been performed for $h = 1/16$ (dash-dotted line), $h = 1/32$ (dashed line) and $h = 1/64$ (full line).

the results indicate, the Uzawa-type method is the computationally most efficient among the three, here, clearly seen in terms of total solution time when direct methods are used to solve the respective subproblems. A similar behaviour can also be expected when iterative solvers of lower complexity replace the direct ones.

5.4. Scaling test. Finally, we present a scaling test demonstrating the convergence behaviour of the preconditioned GMRES and augmented Uzawa-type algorithms with respect to the number of fluid networks n . These methods have been tested for $n = 1, 2, 4, 8$.

In order to perform a reasonable comparison, we have assumed that all network transfer coefficients are equal to 0 irrelevant to the number of networks, $\lambda = 10^3$, $R_i^{-1} = 10^4$, $\alpha_{p_i} = 10^{-4}$, $i = 1, \dots, n$. The test setting is similar to those

TABLE 2. Reference values of model parameters for the four-network MPET model.

parameter	value	unit
λ	505	Nm^{-2}
μ	216	Nm^{-2}
$c_{p_1} = c_{p_2} = c_{p_3} = c_{p_4}$	$4.5 * 10^{-10}$	N^{-1}m^2
$\alpha_1 = \alpha_2 = \alpha_3 = \alpha_4$	0.99	
$\beta_{12} = \beta_{24}$	$1.5 * 10^{-19}$	$\text{N}^{-1}\text{m}^2\text{s}^{-1}$
β_{23}	$2.0 * 10^{-19}$	$\text{N}^{-1}\text{m}^2\text{s}^{-1}$
β_{34}	$1.0 * 10^{-13}$	$\text{N}^{-1}\text{m}^2\text{s}^{-1}$
$K_1 = K_2 = K_4 = K$	$3.75 * 10^{-6}$	$\text{N}^{-1}\text{m}^4\text{s}^{-1}$
K_3	$1.57 * 10^{-9}$	$\text{N}^{-1}\text{m}^4\text{s}^{-1}$

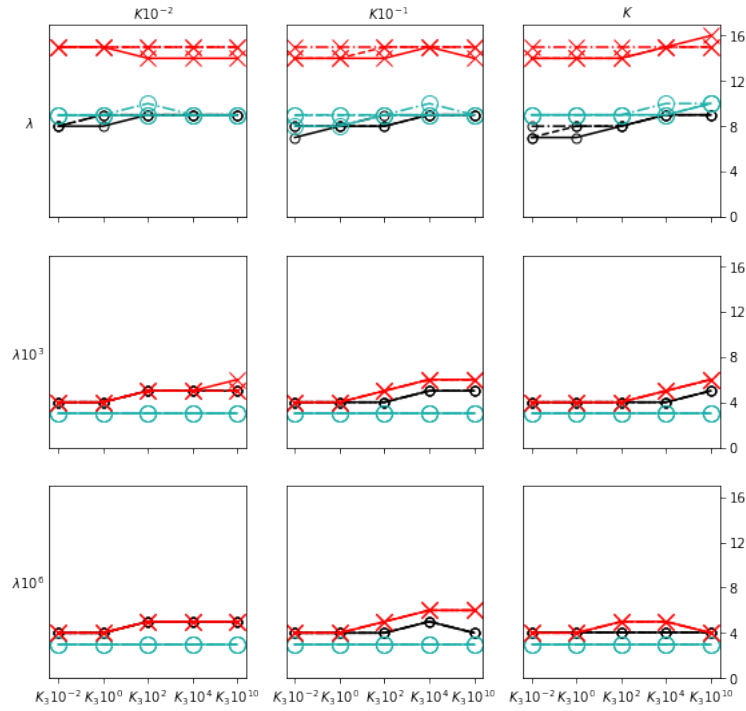


FIGURE 5. Number of preconditioned GMRES (small black circles), fixed-stress split (big green circles) and augmented Uzawa-type (red crosses) iterations for preconditioned residual reduction by a factor 10^8 when solving the four-network MPET problem. These tests have been performed for $h = 1/16$ (dash-dotted line), $h = 1/32$ (dashed line) and $h = 1/64$ (full line).

of the previously considered Biot-Barenblatt and four-network models, i.e., $\partial\Omega = \bar{\Gamma}_1 \cup \bar{\Gamma}_2 \cup \bar{\Gamma}_3 \cup \bar{\Gamma}_4$ with $\Gamma_1, \Gamma_2, \Gamma_3, \Gamma_4$ being the bottom, right, top and left boundaries respectively, $\mathbf{u} = 0$ on Γ_4 , $(\boldsymbol{\sigma} - \sum_{i=1}^n p_i \mathbf{I})\mathbf{n} = (0, 0)^T$ on $\Gamma_1 \cup \Gamma_2$, $(\boldsymbol{\sigma} - \sum_{i=1}^n p_i \mathbf{I})\mathbf{n} = (0, -1)^T$ on Γ_3 and $p_i = 10$, $i = 1, \dots, n$ on Γ . As previously, all the right-hand sides have been chosen to be zero.

TABLE 3. Computational times in seconds for the preconditioned GMRES (t_G), fixed-stress split (t_F) and augmented Uzawa-type (t_U) algorithms to reach preconditioned residual reduction by a factor 10^8 in the norm induced by the preconditioner when solving the four-network MPET problem on a mesh with $h = 1/64$.

		$K_3 \cdot 10^{-2}$			K_3			$K_3 \cdot 10^2$			$K_3 \cdot 10^4$			$K_3 \cdot 10^{10}$		
		t_G	t_F	t_U	t_G	n_F	t_U	t_G	t_F	t_U	t_G	t_F	t_U	t_G	t_F	t_U
λ	$K \cdot 10^{-2}$	15.54	8.98	7.26	15.39	9.12	7.21	15.51	9.09	7.16	15.90	9.17	7.21	15.83	9.33	7.24
	K	15.32	9.20	7.68	15.60	9.13	7.66	15.40	8.91	7.13	15.75	9.12	7.41	16.09	9.26	7.68
	$K \cdot 10^2$	15.25	9.17	7.53	15.47	9.27	7.19	15.24	9.08	7.52	15.44	9.11	7.28	15.64	9.17	7.37
$\lambda \cdot 10^3$	$K \cdot 10^{-2}$	14.87	7.80	5.45	15.00	7.74	5.68	14.95	7.56	5.93	15.16	8.05	5.48	15.31	8.64	6.10
	K	14.71	7.78	5.38	14.81	7.91	5.42	14.74	8.10	5.75	15.05	8.03	6.68	15.23	8.07	6.05
	$K \cdot 10^2$	14.92	8.91	6.78	14.97	8.92	6.69	14.90	8.80	6.96	14.83	8.64	5.21	14.87	9.27	5.28
$\lambda \cdot 10^6$	$K \cdot 10^{-2}$	14.98	8.95	6.14	15.02	9.06	7.07	14.81	7.67	7.12	14.75	7.65	5.90	14.96	7.53	5.81
	K	14.91	8.89	5.40	15.08	8.96	5.61	15.12	9.03	7.01	15.06	9.12	6.33	15.19	9.32	6.20
	$K \cdot 10^2$	14.72	9.27	4.92	14.88	8.99	5.00	15.09	8.96	5.26	15.52	9.19	5.40	15.12	9.24	5.54

We have conducted the numerical tests on a mesh with a mesh-size $h = 1/32$. In all test cases, the number of required iterations to reach a preconditioned residual reduction by a factor 10^8 equals 4. This clearly indicates the robustness of the proposed algorithms with respect to the number of networks as suggested by our theoretical findings.

6. CONCLUDING REMARKS

The main contribution of this manuscript is the development of a new augmented Lagrangian Uzawa algorithm for three-by-three double saddle point block systems arising in Biot's and multiple network poroelasticity models. The proposed method fully decouples the fluid velocity, fluid pressure and solid displacement fields, contrary to the fixed-stress iterative scheme, which decouples only the flow from the mechanics problem. In this manner the subsystems that need to be solved in every iteration become considerably smaller, especially in the models where multiple fluid networks are present.

The presented convergence analysis proves the parameter-robust linear convergence of the new algorithm and additionally offers explicit formulas for a proper choice of required stabilization parameters. All numerical tests confirm the robustness and efficiency of the new fully decoupled iterative scheme and also its superiority in terms of computational work over existing methods.

REFERENCES

1. J.H. Adler, F.J. Gaspar, X. Hu, C. Rodrigo, and L.T. Zikatanov, *Robust block preconditioners for Biot's model*, Domain Decomposition Methods in Science and Engineering XXIV. DD 2017. Lecture Notes in Computational Science and Engineering, vol. 125, Springer, Cham, 2019, pp. 3–16.
2. T. Almani, K. Kumar, A. Dogru, G. Singh, and M.F. Wheeler, *Convergence analysis of multirate fixed-stress split iterative schemes for coupling flow with geomechanics*, Comput. Methods Appl. Mech. Engrg. **311** (2016), 180–207.
3. T. Almani, K. Kumar, and M.F. Wheeler, *Convergence and error analysis of fully discrete iterative coupling schemes for coupling flow with geomechanics*, Comput. Geosci. **21** (2017), 1157–1172.
4. M.S. Alnæs, J. Blechta, J. Hake, A. Johansson, B. Kehlet, A. Logg, C. Richardson, J. Ring, M.E. Rognes, and G.N. Wells, *The fenics project version 1.5*, Archive of Numerical Software **3** (2015), no. 100, 9–23.
5. D. Arnold, R. Falk, and R. Winther, *Preconditioning in $H(\text{div})$ and applications*, Mathematics of Computation **66** (1997), no. 219, 957–984.

6. T. Bærlund, J.J. Lee, K.-A. Mardal, and R. Winther, *Weakly imposed symmetry and robust preconditioners for Biot's consolidation model*, Comput. Methods Appl. Math. **17** (2017), no. 3, 377–396. MR 3667080
7. M. Bai, D. Elsworth, and J.-C. Roegiers, *Multiporosity/multipermeability approach to the simulation of naturally fractured reservoirs*, Water Resources Research **29** (1993), no. 6, 1621–1633.
8. G.I. Barenblatt, G.I. Zheltov, and I.N. Kochina, *Basic concepts in the theory of seepage of homogeneous liquids in fissured rocks [strata]*, J. Appl. Math. Mech. **24** (1960), no. 5.
9. M. Bause, F.A. Radu, and U. Köcher, *Space-time finite element approximation of the Biot poroelasticity system with iterative coupling*, Comput. Methods Appl. Mech. Engrg. **320** (2017).
10. M. Benzi and F.P.A. Beik, *Iterative methods for double saddle point systems*, SIAM J. Matrix Anal. Appl. **39** (2018), no. 2, 902–921.
11. ———, *Uzawa-type and augmented lagrangian methods for double saddle point systems*, Structured Matrices in Numerical Linear Algebra (Prof. Dario Andrea Bini, Prof. Fabio Di Benedetto, Prof. Eugene Tyrtyshnikov, and Prof. Marc Van Barel, eds.), Springer International Publishing, 2019.
12. M.A. Biot, *General theory of three-dimensional consolidation*, J. Appl. Phys. **12** (1941), no. 2, 155–164.
13. ———, *Theory of elasticity and consolidation for a porous anisotropic solid*, J. Appl. Phys. **26** (1955), no. 2, 182–185.
14. D. Boffi, M. Botti, and D.A. Di Pietro, *A nonconforming high-order method for the Biot problem on general meshes*, SIAM Journal on Scientific Computing **38** (2016), no. 3, A1508–A1537.
15. D. Boffi, F. Brezzi, and M. Fortin, *Mixed finite element methods and applications*, Springer Ser. Comput. Math., vol. 44, Springer, Heidelberg, 2013.
16. J. W. Both, M. Borregales, J.M. Nordbotten, K. Kumar, and F.A. Radu, *Robust fixed stress splitting for Biot's equations in heterogeneous media*, Appl. Math. Lett. **68** (2017).
17. J.W. Both, K. Kumar, J.M. Nordbotten, and F.A. Radu, *Anderson accelerated fixed-stress splitting schemes for consolidation of unsaturated porous media*, Comput. Math. Appl. **77** (2018).
18. F. Brezzi, *On the existence, uniqueness and approximation of saddle-point problems arising from Lagrangian multipliers*, Rev. Française Automat. Informat. Recherche Opérationnelle Sér. Rouge **8** (1974), no. R-2, 129–151.
19. Mats Kirkesther Brun, Elyes Ahmed, Inga Berre, Jan Martin Nordbotten, and Florin Adrian Radu, *Monolithic and splitting based solution schemes for fully coupled quasi-static thermo-poroelasticity with nonlinear convective transport*, 2019.
20. D. Chou, J.C. Vardakis, L. Guo, B.J. Tully, and Y. Ventikos, *A fully dynamic multi-compartmental poroelastic system: Application to aqueductal stenosis*, J. Biomech. **49** (2016), 2306–2312.
21. M. Costabel and M. Dauge, *On the inequalities of Babuška-Aziz, Friedrichs and Horgan-Payne*, Arch. Rational Mech. Anal. **217** (2015), 873–898.
22. S. Dana and M.F. Wheeler, *Convergence analysis of two-grid fixed stress iterative scheme for coupled flow and deformation in heterogeneous poroelastic media*, Comput. Methods Appl. Mech. Engrg. **341** (2018).
23. National Agency for Finite Element Methods & Standards (Great Britain), *The standard nafems benchmarks*, Glasgow: NAFEMS, 1990.
24. L. Guo, Z. Li, J. Lyu, Y. Mei, J. Vardakis, D. Chen, C. Han, X. Lou, and Y. Ventikos, *On the validation of a multiple-network poroelastic model using arterial spin labeling MRI data*, Frontiers in Computational Neuroscience **13** (2019).
25. L. Guo, J.C. Vardakis, T. Lassila, M. Mitolo, N. Ravikumar, D. Chou, M. Lange, A. Sarrami-Foroushani, B.J. Tully, Z.A. Taylor, S. Varma, A. Venneri, A.F. Frangi, and Y. Ventikos, *Subject-specific multi-poroelastic model for exploring the risk factors associated with the early stages of alzheimer's disease*, Interface Focus **8** (2018), no. 1, 20170019.
26. R. Hiptmair and J. Xu, *Nodal auxiliary space preconditioning in $H(\text{curl})$ and $H(\text{div})$ spaces*, SIAM Journal on Numerical Analysis **45** (2007), no. 6, 2483–2509 (electronic).
27. Q. Hong and J. Kraus, *Parameter-robust stability of classical three-field formulation of Biot's consolidation model*, Electron. Trans. Numer. Anal. **48** (2018), 202–226.
28. Q. Hong, J. Kraus, M. Lymbery, and F. Philo, *Conservative discretizations and parameter-robust preconditioners for Biot and multiple-network flux-based poroelasticity models*, Numer. Linear Algebra with Appl.; e2242 (2019), see also arXiv:1806.00353v2.
29. Q. Hong, J. Kraus, M. Lymbery, and M. F. Wheeler, *Parameter-robust convergence analysis of fixed-stress split iterative method for multiple-permeability poroelasticity systems*, Multiscale Modeling & Simulation **18** (2020), no. 2, 916–941.
30. Q. Hong, J. Kraus, J. Xu, and L. Zikatanov, *A robust multigrid method for discontinuous Galerkin discretizations of Stokes and linear elasticity equations*, Numer. Math. **132** (2016), no. 1, 23–49.
31. X. Hu, C. Rodrigo, F.J. Gaspar, and L.T. Zikatanov, *A nonconforming finite element method for the Biot's consolidation model in poroelasticity*, J. Comput. Appl. Math. **310** (2017), 143–154.
32. G. Kanschat and B. Riviere, *A finite element method with strong mass conservation for Biot's linear consolidation model*, Journal of Scientific Computing **77** (2018), no. 3, 1762–1779.
33. J. Kim, H.A. Tchelepi, and R. Juanes, *Stability, accuracy and efficiency of sequential methods for coupled flow and geomechanics*, SPE Journal **16** (2011), no. 2.

34. A.E. Kolesov and P.N. Vabishchevich, *Splitting schemes with respect to physical processes for double-porosity poroelasticity problems*, Russ. J. Numer. Anal. Math. Model. **32** (2017).
35. J. Kraus, R. Lazarov, M. Lymbery, S. Margenov, and L. Zikatanov, *Preconditioning heterogeneous $H(\text{div})$ problems by additive Schur complement approximation and applications*, SIAM Journal on Scientific Computing **38** (2016), no. 2, A875–A898.
36. J.J. Lee, *Robust error analysis of coupled mixed methods for Biot’s consolidation model*, J. Sci. Comput. **69** (2016), no. 2, 610–632.
37. J.J. Lee, K.-A. Mardal, and R. Winther, *Parameter-robust discretization and preconditioning of Biot’s consolidation model*, SIAM J. Sci. Comput. **39** (2017), no. 1, A1–A24.
38. J.J. Lee, E. Piersanti, K.-A. Mardal, and M.E. Rognes, *A mixed finite element method for nearly incompressible multiple-network poroelasticity*, SIAM Journal on Scientific Computing **41** (2019), no. 2, A722–A747.
39. Y. J. Lee, J. Wu, and L. Xu, J. Zikatanov, *Robust subspace correction methods for nearly singular systems*, Mathematical Models and Methods in Applied Sciences **17** (2007), no. 11, 1937–1963.
40. Y.J. Lee, J. Wu, and J. Chen, *Robust multigrid method for the planar linear elasticity problems*, Numerische Mathematik **113** (2009), no. 3, 473–496.
41. Y.J. Lee, J. Wu, J. Xu, and L. Zikatanov, *A sharp convergence estimate for the method of subspace corrections for singular systems of equations*, Mathematics of Computation **77** (2008), no. 262, 831.
42. A. Logg, K.-A. Mardal, G.N. Wells, et al., *Automated solution of differential equations by the finite element method*, Springer, 2012.
43. K.-A. Mardal and R. Winther, *Preconditioning discretizations of systems of partial differential equations*, Numer. Linear Algebra Appl. **18** (2011), no. 1, 1–40.
44. A. Mikić and M.F. Wheeler, *Convergence of iterative coupling for coupled flow and geomechanics*, Comput. Geosci. **17** (2013).
45. R. Oyarzúa and R. Ruiz-Baier, *Locking-free finite element methods for poroelasticity*, SIAM J. Numer. Anal. **54** (2016), no. 5, 2951–2973.
46. C. Rodrigo, X. Hu, P. Ohm, J.H. Adler, F.J. Gaspar, , and L.T. Zikatanov, *New stabilized discretizations for poroelasticity and the Stokes’ equations*, Computer Methods in Applied Mechanics and Engineering **341** (2018), 467–484.
47. J. Schöberl, *Multigrid methods for a parameter dependent problem in primal variables*, Numerische Mathematik **84** (1999), no. 1, 97–119.
48. R.E. Showalter, *Poroelastic filtration coupled to Stokes flow*, Lecture Notes in Pure and Appl. Math. **242** (2010), 229–241.
49. J. Sogn and W. Zulehner, *Schur complement preconditioners for multiple saddle point problems of block tridiagonal form with application to optimization problems*, IMA J. Numer. Anal. **39** (2019), 1328–1359.
50. E. Størvik, J.W. Both, K. Kumar, J.M. Nordbotten, and F.A. Radu, *On the optimization of the fixed-stress splitting for Biot’s equations*, Int. J. Numer. Meth. Eng. (2019).
51. B. Tully and Y. Ventikos, *Cerebral water transport using multiple-network poroelastic theory: application to normal pressure hydrocephalus*, J. Fluid Mech. **667** (2011), 188–215.
52. J. C. Vardakis, L. Guo, T. W. Peach, T. Lassila, M. Mitolo, D. Chou, and et al., *Fluid-structure interaction for highly complex, statistically defined, biological media: homogenisation and a 3d multi-compartmental poroelastic model for brain biomechanics*, J. Fluids Struct. (2019).
53. J.C. Vardakis, D. Chou, B.J. Tully, C.C. Hung, T.H. Lee, P.H. Tsui, and Y. Ventikos, *Investigating cerebral oedema using poroelasticity*, Med. Eng. Phys. **38** (2016), no. 1, 48–57.
54. J.C. Vardakis, B.J. Tully, and Y. Ventikos, *Exploring the efficacy of endoscopic ventriculostomy for hydrocephalus treatment via a multicompartmental poroelastic model of CSF transport: A computational perspective*, PLoS ONE **8** (2013), no. 12, e84577.
55. P. S. Vassilevski and R. D. Lazarov, *Preconditioning mixed finite element saddle-point elliptic problems*, Numer. Linear Algebra with Appl. **3** (1996), no. 1, 1–20.
56. J.A. White, N. Castelletto, and H.A. Tchelepi, *Block-partitioned solvers for coupled poromechanics: A unified framework*, Comput. Methods Appl. Mech. Engrg. **303** (2016), 55–74.
57. J. Xu, *Iterative methods by space decomposition and subspace correction*, SIAM Rev. (1992), no. 4, 581–613.
58. J. Xu and L. Zikatanov, *The method of alternating projections and the method of subspace corrections in Hilbert space*, Journal of the American Mathematical Society **15** (2002), no. 3, 573–597.